TABLE 3
Replication of HIV-1 containing a random combination of the eight amino acid substitutions from HIV-$1_{V3L\#08}$ V3 loop in PM1 and PM1/CCR5 cells

Viral clone	V3 loop sequence	p24 Gag (ng/ml)[a] PM1	PM1/CCR5	Ratio[b]
HIV-$1_{JR-FLan}$	CTRPNNNTRKSIHIGPGRAFYTTGEIIGDIRQAHC	140	270	1.9
HIV-$1_{V3L\#08}$	.....VTM.....L.A..DV..N.....	83	8.0	< 0.1
HIV-$1_{V3L\#102}$	.....T.....L.....N.....	200	72	0.4
HIV-$1_{V3L\#103}$	.....TM.....DV.....	150	<1.0	< 0.1
HIV-$1_{V3L\#104}$	.....VT.....A..DV..N.....	210	84	0.4
HIV-$1_{V3L\#117}$	.....VT.....L.A...V.....	110	<1.0	< 0.1
HIV-$1_{V3L\#121}$	.....VT.....L.....V.....	120	<1.0	< 0.1
HIV-$1_{V3L\#124}$	.....TM.....A..DV.....	150	40	0.3
HIV-$1_{V3L\#125}$	.....T.....A.....	14	170	11
HIV-$1_{V3L\#127}$	.....VTM.....L.A.....N.....	200	<1.0	< 0.1
HIV-$1_{V3L\#128}$	.....VT.....L.A..D...N.....	160	30	0.2
HIV-$1_{V3L\#130}$	.....M.....A..D...N.....	130	180	1.4
HIV-$1_{V3L\#132}$	.....TM.....V.....	160	70	0.4
HIV-$1_{V3L\#133}$	.....VT.....A...V..N.....	120	20	0.2

[a] PM1 or PM1/CCR5 cells (4×10^4) were infected with each virus (8 ng of p24 Gag). On day 6 the extent of viral replication was measured by p24 Gag antigen ELISA. Results represent the average of three independent experiments.
[b] Ratio, the concentration of p24 Gag in the supernatant of PM1/CCR5 cells was divided by that of PM1 cells.

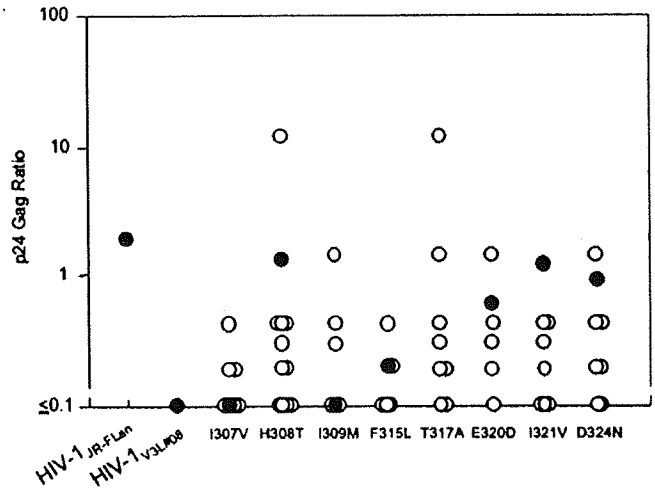

FIGURE 9. **Effect of each amino acid substitution on preferential replication of V3 mutant viruses.** Ratios of p24 Gag in seven mutant viruses in Table 2 and 12 mutant viruses in Table 3 were plotted. *Closed circle*, mutant virus containing one substitution in the V3 loop (Table 2). *Open circle*, virus containing a random combination of multiple substitutions in the HIV-$1_{V3L\#08}$ V3 loop (Table 3).

however, HIV-$1_{V3L\#08}$ showed no CCR5-dependent replication suppression compared with MAGI/CCR5, NP2/CD4/lowCCR5 expressing a similar level of CD4, and a lower level of CCR5 (data not shown). The results suggest that distribution or localization of CCR5 on the surface in PM1 cell line may be distinct from these adherent cells.

Depending on the surface of the host cell, HIV-1 incorporates cell-derived molecules into its envelope (46, 47). HLA-DR, β_2-microglobulin, ICAM-1 (intercellular adhesion molecule 1), and other cellular surface proteins were incorporated into a budding virion (48, 49), whereas CD4, CXCR4, and CCR5 were not detectable (50). Using the anti-CCR5 mAb, T21/8, we found CCR5 incorporated into a budding virion (Fig. 8). In contrast, two anti-CCR5 mAbs, 2D7 and 3A9, failed to capture virions from PM1 and PM1/CCR5 cells despite the fact that 2D7 (Fig. 2) and 3A9 (data not shown) could recognize CCR5 at the cell surface, indicating that the epitopes of 2D7 and 3A9 were lost by conformation change or concealed from the antibodies by interaction with other molecule(s) on a virus particle. The epitope of 2D7 is mapped to the second extracellular loop including Lys^{171}-Glu^{172} by alanine mutagenesis scan (44). The tertiary structure of CCR5 including Ser^7 and $^9IYD^{11}$ in the N terminus and His^{88} and Trp^{94} in the first extracellular loop are estimated to contribute to the binding of 3A9 by phage displayed peptide libraries (45), whereas T21/8 epitope has not been mapped but should be located in the N terminus of 22 amino acid residues from Met^1 to Lys^{22}; T21/8 was raised against a peptide corresponding to residues 1–22 of CCR5 according to the manufacturer. For viral entry, binding of coreceptors to HIV-1 gp120 is mediated by the V3 loop and the coreceptor-binding site located in the bridging sheet of gp120 (12, 14–16). The N terminus and the first and second extracellular loops of CCR5 are thought to interact with gp120 (51, 52). Loss of 2D7 and 3A9 binding with CCR5 at the viral envelope indicate that conformation of CCR5 at the viral envelope is distinct from that of CCR5 at the host cell surface.

The following scenario could explain the decreased infectivity in HIV-$1_{V3L\#08}$ from PM1/CCR5 cells. In HIV-$1_{V3L\#08\text{-}A69T}$, HIV-$1_{JR\text{-}FLan}$, and HIV-$1_{JR\text{-}FLan\text{-}A69T}$ generated from PM1 and PM1/CCR5 cells, cellular CCR5 is incorporated into the virion envelope but does not impair viral infectivity due to the low level of CCR5. A similar amount of CCR5 incorporated into HIV-$1_{V3L\#08}$ from PM1 cells is not sufficient to impair viral

infectivity either. Larger amounts of CCR5 are recruited by HIV-$1_{V3L\#08}$ from the PM1/CCR5 cell surface into the virions, and the CCR5 levels are above the threshold needed for suppression of viral replication. HIV-$1_{V3L\#08}$ from PM1/CCR5 cells was almost completely precipitated by T21/8, indicating that most of the virus particles contained sufficient levels of CCR5 for capture (Fig. 8*B*), although immunoprecipitation efficiency of virions does not proportionally reflect the amount of CCR5. Otherwise incorporated CCR5 may specifically impair gp120 and gp41 function by an unknown mechanism through the HIV-$1_{V3L\#08}$ V3 loop or via recruitment of nonfunctional gp120-CCR5 complexes at the virion surface. Loss of infectivity seems to be V3-dependent (Tables 2 and 3), and amino acid substitutions near the V3 tip may play a pivotal role on the complex-formation on virions. However, the role of the point mutation of C1 in the revertant virus (HIV-$1_{V3L\#08\text{-}A69T}$) on V3 conformation or amount of gp120 and gp41 on virions (Fig. 7) is still murky. Another possibility is that CCR5 interacts with HIV-$1_{V3L\#08}$ gp120 between virus-virus envelopes in the *trans* position without CD4; the interaction between viral particles through CCR5 and gp120 leads to decrease of viral infectivity, although this is unlikely. To further elucidate incorporation of CCR5 into a virus particle and decrease of viral infectivity, the molecular behavior of CCR5 and HIV-$1_{V3L\#08}$ gp120 in PM1/CCR5 cells needs to be studied.

There are several reports for donor-dependent variations in CCR5 expression even among donors who do not possess the CCR5Δ32 allele, with a ~20-fold variation in CCR5 expression on peripheral blood mononuclear cells from human donors being reported (53, 54). CCR5 expression levels in the target cells might be a source of alternative selective pressure on the development of the HIV-1 envelope *in vivo*, although the range of expression from PM1 to PM1/CCR5 cells is supposed to be higher than in CCR5-expressing cells *in vivo*.

Thus, high CCR5 expression does not always benefit replication in all R5 HIV-1. The same V3 loop sequence for the $R5^L$ phenotype, including HIV-$1_{V3L\#08}$, HIV-$1_{V3L\#23}$, and HIV-$1_{V3L\#25}$, could not be found in the data base of HIV-1 clinical isolates, suggesting that HIV-1 has evolved to overcome problems in viral replication caused by the high expression levels of CCR5 in target cells *in vivo*. The results demonstrate the significant implications of an alternative influence of CCR5 on R5 HIV-1 replication.

Acknowledgments—We thank Akiko Honda and Kazuhisa Yoshimura for technical advice on real-time PCR and Tetsuya Kimura for scientific discussion.

REFERENCES

1. Berger, E. A., Doms, R. W., Fenyo, E. M., Korber, B. T., Littman, D. R., Moore, J. P., Sattentau, Q. J., Schuitemaker, H., Sodroski, J., and Weiss, R. A. (1998) *Nature* **391**, 240
2. Doms, R. W., and Peiper, S. C. (1997) *Virology* 235, 179–190
3. Moore, J. P., Trkola, A., and Dragic, T. (1997) *Curr. Opin. Immunol.* 9, 551–562
4. Lin, Y. L., Mettling, C., Portales, P., Reynes, J., Clot, J., and Corbeau, P. (2002) *Proc. Natl. Acad. Sci. U. S. A.* **99**, 15590–15595
5. Peters, P. J., Bhattacharya, J., Hibbitts, S., Dittmar, M. T., Simmons, G., Bell, J., Simmonds, P., and Clapham, P. R. (2004) *J. Virol.* 78, 6915–6926
6. Platt, E. J., Wehrly, K., Kuhmann, S. E., Chesebro, B., and Kabat, D. (1998) *J. Virol.* 72, 2855–2864
7. Reynes, J., Baillat, V., Portales, P., Clot, J., and Corbeau, P. (2003) *J. Acquired Immune Defic. Syndr.* 34, 114–116
8. Walter, B. L., Wehrly, K., Swanstrom, R., Platt, E., Kabat, D., and Chesebro, B. (2005) *J. Virol.* 79, 4828–4837
9. Kwong, P. D., Wyatt, R., Robinson, J., Sweet, R. W., Sodroski, J., and Hendrickson, W. A. (1998) *Nature* **393**, 648–659
10. Trkola, A., Dragic, T., Arthos, J., Binley, J. M., Olson, W. C., Allaway, G. P., Cheng-Mayer, C., Robinson, J., Maddon, P. J., and Moore, J. P. (1996) *Nature* 384, 184–187
11. Wyatt, R., Kwong, P. D., Desjardins, E., Sweet, R. W., Robinson, J., Hendrickson, W. A., and Sodroski, J. G. (1998) *Nature* **393**, 705–711
12. Reeves, J. D., Gallo, S. A., Ahmad, N., Miamidian, J. L., Harvey, P. E., Sharron, M., Pohlmann, S., Sfakianos, J. N., Derdeyn, C. A., Blumenthal, R., Hunter, E., and Doms, R. W. (2002) *Proc. Natl. Acad. Sci. U. S. A.* **99**, 16249–16254
13. Reeves, J. D., Miamidian, J. L., Biscone, M. J., Lee, F. H., Ahmad, N., Pierson, T. C., and Doms, R. W. (2004) *J. Virol.* 78, 5476–5485
14. Rizzuto, C. D., Wyatt, R., Hernandez-Ramos, N., Sun, Y., Kwong, P. D., Hendrickson, W. A., and Sodroski, J. (1998) *Science* 280, 1949–1953
15. Rizzuto, C., and Sodroski, J. (2000) *AIDS Res. Hum. Retroviruses* **16**, 741–749
16. Suphaphiphat, P., Thitithanyanont, A., Paca-Uccaralertkun, S., Essex, M., and Lee, T. H. (2003) *J. Virol.* 77, 3832–3837
17. Wu, L., Gerard, N. P., Wyatt, R., Choe, H., Parolin, C., Ruffing, N., Borsetti, A., Cardoso, A. A., Desjardin, E., Newman, W., Gerard, C., and Sodroski, J. (1996) *Nature* 384, 179–183
18. Wyatt, R., and Sodroski, J. (1998) *Science* 280, 1884–1888
19. Zhang, W., Canziani, G., Plugariu, C., Wyatt, R., Sodroski, J., Sweet, R., Kwong, P., Hendrickson, W., and Chaiken, I. (1999) *Biochemistry* 38, 9405–9416
20. Delwart, E. L., and Panganiban, A. T. (1989) *J. Virol.* 63, 273–280
21. Steck, F. T., and Rubin, H. (1966) *Virology* 29, 628–641
22. Aiken, C., Konner, J., Landau, N. R., Lenburg, M. E., and Trono, D. (1994) *Cell* 76, 853–864
23. Bresnahan, P. A., Yonemoto, W., Ferrell, S., Williams-Herman, D., Geleziunas, R., and Greene, W. C. (1998) *Curr. Biol.* 8, 1235–1238
24. Craig, H. M., Pandori, M. W., and Guatelli, J. C. (1998) *Proc. Natl. Acad. Sci. U. S. A.* 95, 11229–11234
25. Greenberg, M., DeTulleo, L., Rapoport, I., Skowronski, J., and Kirchhausen, T. (1998) *Curr. Biol.* 8, 1239–1242
26. Mangasarian, A., Foti, M., Aiken, C., Chin, D., Carpentier, J. L., and Trono, D. (1997) *Immunity* 6, 67–77
27. Piguet, V., Chen, Y. L., Mangasarian, A., Foti, M., Carpentier, J. L., and Trono, D. (1998) *EMBO J.* 17, 2472–2481
28. Geleziunas, R., Bour, S., and Wainberg, M. A. (1994) *FASEB J.* 8, 593–600
29. Willey, R. L., Maldarelli, F., Martin, M. A., and Strebel, K. (1992) *J. Virol.* 66, 7193–7200
30. Palese, P., Tobita, K., Ueda, M., and Compans, R. W. (1974) *Virology* 61, 397–410
31. Lama, J., Mangasarian, A., and Trono, D. (1999) *Curr. Biol.* 9, 622–631
32. Levesque, K., Zhao, Y. S., and Cohen, E. A. (2003) *J. Biol. Chem.* 278, 28346–28353
33. Michel, N., Allespach, I., Venzke, S., Fackler, O. T., and Keppler, O. T. (2005) *Curr. Biol.* 15, 714–723
34. Yusa, K., Maeda, Y., Fujioka, A., Monde, K., and Harada, S. (2005) *J. Biol. Chem.* 280, 30083–30090
35. Lusso, P., Cocchi, F., Balotta, C., Markham, P. D., Louie, A., Farci, P., Pal, R., Gallo, R. C., and Reitz, M. S., Jr. (1995) *J. Virol.* 69, 3712–3720
36. Maeda, Y., Foda, M., Matsushita, S., and Harada, S. (2000) *J. Virol.* 74, 1787–1793
37. Hachiya, A., Aizawa-Matsuoka, S., Tanaka, M., Takahashi, Y., Ida, S., Gatanaga, H., Hirabayashi, Y., Kojima, A., Tatsumi, M., and Oka, S. (2001) *Antimicrob. Agents Chemother.* 45, 495–501
38. Mariani, R., Rutter, G., Harris, M. E., Hope, T. J., Krausslich, H. G., and

Landau, N. R. (2000) *J. Virol.* **74**, 3859–3870
39. Kimpton, J., and Emerman, M. (1992) *J. Virol.* **66**, 2232–2239
40. Esser, M. T., Graham, D. R., Coren, L. V., Trubey, C. M., Bess, J. W., Jr., Arthur, L. O., Ott, D. E., and Lifson, J. D. (2001) *J. Virol.* **75**, 6173–6182
41. Inudoh, M., Kato, N., and Tanaka, Y. (1998) *Microbiol. Immunol.* **42**, 875–877
42. Cantin, R., Fortin, J. F., Lamontagne, G., and Tremblay, M. (1997) *Blood* **90**, 1091–1100
43. Cantin, R., Fortin, J. F., Lamontagne, G., and Tremblay, M. (1997) *J. Virol.* **71**, 1922–1930
44. Lee, B., Sharron, M., Blanpain, C., Doranz, B. J., Vakili, J., Setoh, P., Berg, E., Liu, G., Guy, H. R., Durell, S. R., Parmentier, M., Chang, C. N., Price, K., Tsang, M., and Doms, R. W. (1999) *J. Biol. Chem.* **274**, 9617–9626
45. O'Connor, K. H., Konigs, C., Rowley, M. J., Irving, J. A., Wijeyewickrema, L. C., Pustowka, A., Dietrich, U., and Mackay, I. R. (2005) *J. Immunol. Methods* **299**, 21–35
46. Ott, D. E. (2002) *Rev. Med. Virol.* **12**, 359–374
47. Tremblay, M. J., Fortin, J. F., and Cantin, R. (1998) *Immunol. Today* **19**, 346–351
48. Hoxie, J. A., Fitzharris, T. P., Youngbar, P. R., Matthews, D. M., Rackowski, J. L., and Radka, S. F. (1987) *Hum. Immunol.* **18**, 39–52
49. Ott, D. E. (1997) *Rev. Med. Virol.* **7**, 167–180
50. Lallos, L. B., Laal, S., Hoxie, J. A., Zolla-Pazner, S., and Bandres, J. C. (1999) *AIDS Res. Hum. Retroviruses* **15**, 895–897
51. Dragic, T., Trkola, A., Lin, S. W., Nagashima, K. A., Kajumo, F., Zhao, L., Olson, W. C., Wu, L., Mackay, C. R., Allaway, G. P., Sakmar, T. P., Moore, J. P., and Maddon, P. J. (1998) *J. Virol.* **72**, 279–285
52. Farzan, M., Choe, H., Vaca, L., Martin, K., Sun, Y., Desjardins, E., Ruffing, N., Wu, L., Wyatt, R., Gerard, N., Gerard, C., and Sodroski, J. (1998) *J. Virol.* **72**, 1160–1164
53. Moore, J. P. (1997) *Science* **276**, 51–52
54. Wu, L., Paxton, W. A., Kassam, N., Ruffing, N., Rottman, J. B., Sullivan, N., Choe, H., Sodroski, J., Newman, W., Koup, R. A., and Mackay, C. R. (1997) *J. Exp. Med.* **185**, 1681–1691

Cellular Microbiology (2007) 9(1), 196–203

doi:10.1111/j.1462-5822.2006.00781.x
First published online 10 August 2006

A broad antiviral neutral glycolipid, fattiviracin FV-8, is a membrane fluidity modulator

Shinji Harada,[1]* Kazumi Yokomizo,[2] Kazuaki Monde,[1] Yosuke Maeda[1] and Keisuke Yusa[1]

[1]*Department of Medical Virology, Graduate School of Medical Sciences, Kumamoto University, Kumamoto 860-8556, Japan.*

[2]*Faculty of Pharmaceutical Science, Sojo University, Kumamoto 860-0082, Japan.*

Summary

To screen for an effective antiviral compound which acts as a membrane fluidity modulator, dichotomous effects on human immunodeficiency virus type 1 (HIV-1) infection due to different treatments of several glycolipids and lipids were examined. Continuous treatment of infected cells with 40 μg ml^{-1} fattiviracin FV-8, a neutral glycolipid isolated from *Streptomycetes*, inhibited HIV-1 infection by 96%, whereas pretreatment with 400 μg ml^{-1} enhanced infectivity 4.7-fold. The glycolipid showed similar effects as glycyrrhizin; it inhibited infection by broad enveloped viruses, blocked cell–cell fusion, reduced the infectivity of treated virions and enhanced susceptibility to viral infection and cell–cell fusion of cells pretreated with high doses of the compound. Suppression and enhancement was correlated with decreased and increased fluidity of plasma membrane of the fattiviracin FV-8-treated cells. Restricted movement of membrane molecules might impede the formation of a wide fusion pore, and therefore be critical to the entry of viruses. Thus, this can be applied as a new strategy to inhibit viral infections.

Introduction

Fusion is used by many enveloped viruses to gain entry into cells. Fusion actually encompasses many different processes, such as conformational changes of the viral glycoprotein spike by binding to receptor(s) or low pH in the endosome, exposing hydrophobic fusion peptides (fusion-activated domain) and trimers formed from helical coiled-coil rods (Colman and Lawrence, 2003) or a β-sheet loop (Gibbons *et al.*, 2004; Modis *et al.*, 2004). One of the common fusion processes among enveloped viruses is fluidity-mediated accumulation of fusion-activated domains whereby the plasma membrane and viral envelope form a wide fusion pore large enough for a viral core to pass through (Plonsky and Zimmerberg, 1996; Roche and Gaudin, 2002; Gibbons *et al.*, 2003; Harada *et al.*, 2004a,b).

Correlation between HIV-1 infectivity and membrane fluidity was observed; namely a 5% decrease in fluidity suppressed HIV-1 infectivity by 56%, whereas a 5% increase enhanced infectivity 2.4-fold (Harada *et al.*, 2005). Glycyrrhizin with hydrophilic and lipophilic domains decreased or increased membrane fluidity depending on continuous treatment or pretreatment, respectively, of cells, which correlated with suppression or enhancement of HIV-1 infectivity and cell–cell fusion activity (Harada, 2005). Glycyrrhizin acts as a fluidity modulator probably due to its simple diffusion in and out of lipid bilayer membranes, thus showing broad antiviral activity especially against enveloped viruses. However, a disadvantage of the glycyrrhizin is that a high concentration (500 μg ml^{-1}) of the compound is needed to suppress viral infections. Thus, a more effective modulator is required.

It is hypothesized that glycolipids could exert the same pharmacodynamic action on the lipid bilayer membrane as glycyrrhizin, because glycolipids are amphipathic with hydrophilic sugar and lipophilic lipid structures. In order to evaluate the effectiveness of a number of compounds in blocking HIV-1 infection by decreasing membrane fluidity, it was necessary to develop a screening system, which was highly reproducible and convenient for parallel evaluation. In this paper, we screened accessible glycolipid compounds as membrane fluidity modulators to seek an effective antiviral agent and used lipids as a control. We found one (fattiviracin FV-8) consisting of high-molecular-weight glycolipids that showed strong anti-HIV-1 activity by suppressing membrane fluidity. We propose that some of the glycolipids could be used as antiviral agents through a new mechanism of blocking fusion-pore-formation.

Received 16 March, 2006; revised 8 June, 2006; accepted 29 June, 2006. *For correspondence. E-mail biodef@gpo.kumamoto-u.ac.jp; Tel. (+81) 96 3735128; Fax (+81) 96 3735132.

Table 1. Effect of lipids and glycolipids on HIV-1 infection.

Agents (MW)	% infection[a] of X4 HIV-1 by	
	Pretreatment of cells[b]	Continuous treatment[c]
I. Lipids		
Sphingomyelin	NT	> 80
Sphingosine	NT	> 80
Lysophosphatidic acid	< 120	> 80
II. Glycolipids		
Galactosylceramide (< 920)	200	70
Monosialoganglioside GM_1	< 120	66
Capsianoside II (1084)	143	61
Capsianoside XI (922)	150	78
Capsianoside G (1402)	819	9
Capsianoside A (1562)	210	43
Fattiviracin FV-8 (1432)	473	4

a. Percentage infection; (% positive cells in test/% positive cells in control) × 100.
b. 400 μg ml^{-1} of each agent was used.
c. 40 μg ml^{-1} of each agent was used.
NT; not tested.

Results and discussion

Screening of lipids and glycolipids as membrane fluidity modulators

As dichotomous (inhibitory and enhanced) effects of glycyrrhizin on HIV-1 infection well reflected changes in membrane fluidity (Harada, 2005) and could be conveniently assessed by infection of MAGI/CCR5 cells with LAI (X4) HIV-1, a number of lipids and glycolipids were screened with this system (Table 1). The cells were mixed with viruses and 40 μg ml^{-1} of each compound, cultured for 2 days (continuous treatment) and were stained to detect HIV-1-positive cells by multinuclear activation of a galactosidase indicator (MAGI) assay (Kimpton and Emerman, 1992). Table 1 shows that the lipids had no effect (less than 20% inhibition), while glycolipids exhibited 22–96% inhibition of HIV-1 infection. Capsianosides were extracted from *Capsicum annuum*. Capsianosides II and XI were identified as monomeric compounds of acylic diterpene glycoside, and G and A as esters of the acylic diterpene glycoside (Song *et al.*, 2001). Capsianosides II and A have a longer glucose chain than XI and G. A neutral glycolipid, named fattiviracin FV-8 that was isolated from *Streptomycetes* is a macrocyclic diester consisting of four D-glucose units and two (C_{24} and C_{33}) hydroxy fatty acids (Uyeda *et al.*, 1998). Fattiviracin FV-8 has the same macrocyclic diester structure as cycloviracins B_1 and B_2 (Tsunakawa *et al.*, 1992a,b). When the cells were treated with 400 μg ml^{-1} of each glycolipid at 37°C for 1 h, washed once with medium (pretreatment) and subjected to HIV-1 infection, all except monosialoganglioside GM_1 showed enhanced susceptibility to HIV-1 infection. Among them, compounds with higher molecular weight and fewer sugars (e.g. capsianoside G and fattiviracin FV-8) tended to exhibit more inhibitory and stimulatory effects on HIV-1 infection. In particular, fattiviracin FV-8 showed 96% inhibition and 4.7-fold enhancement of HIV-1 infectivity. Thus, we further explored and clarified how fattiviracin FV-8 acts on HIV-1 infection.

Inhibitory effects of fattiviracin FV-8 on HIV-1 infection by continuous treatment

Fattiviracin FV-8 has been reported to show potent antiviral activity against herpes simplex virus, varicella-zoster virus and influenza A virus as well as HIV-1 (Yokomizo *et al.*, 1998; Habib *et al.*, 2001). The effect of fattiviracin FV-8 on LAI (X4), JR-FL (R5) and 89.6 (X4R5) HIV-1 infection was reassessed when MAGI/CCR5 cells were treated with mixtures of each virus with the diluted glycolipid. The compound inhibited all strains in a dose-dependent manner; 50% and 90% effective concentrations (EC_{50} and EC_{90}) to each strain were observed at about 6.25 μg ml^{-1} and 25 μg ml^{-1} respectively (Fig. 1A). Therefore, the inhibitory effect of the fattiviracin FV-8 was not dependent on the viral strain. The concentration required to inhibit 50% of MAGI/CCR5 cell growth (CC_{50}) by continuous treatment was 280 μg ml^{-1}. Fattiviracin FV-8 weakly inhibited viral adsorption dose-dependently (Fig. 1B) by measuring the amount of p24 bound on cells. Fifty per cent inhibition of viral binding to cells occurred at 50 μg ml^{-1}, at which concentration more than 95% of viral infection was inhibited (Fig. 1A). Thus, inhibition of viral attachment by fattiviracin FV-8 was not parallel to the inhibition of viral infectivity. To analyse the time-dependent effect of fattiviracin FV-8, the glycolipid was added at 0, 1 and 3 h after inoculation of X4 HIV-1 to MAGI/CCR5 cells to obtain a final concentration of 12.5 μg ml^{-1}. The per cent infection at 0, 1 and 3 h were 16.5%, 66.0% and 87.8% respectively (Fig. 1C). As we previously reported (Habib *et al.*,

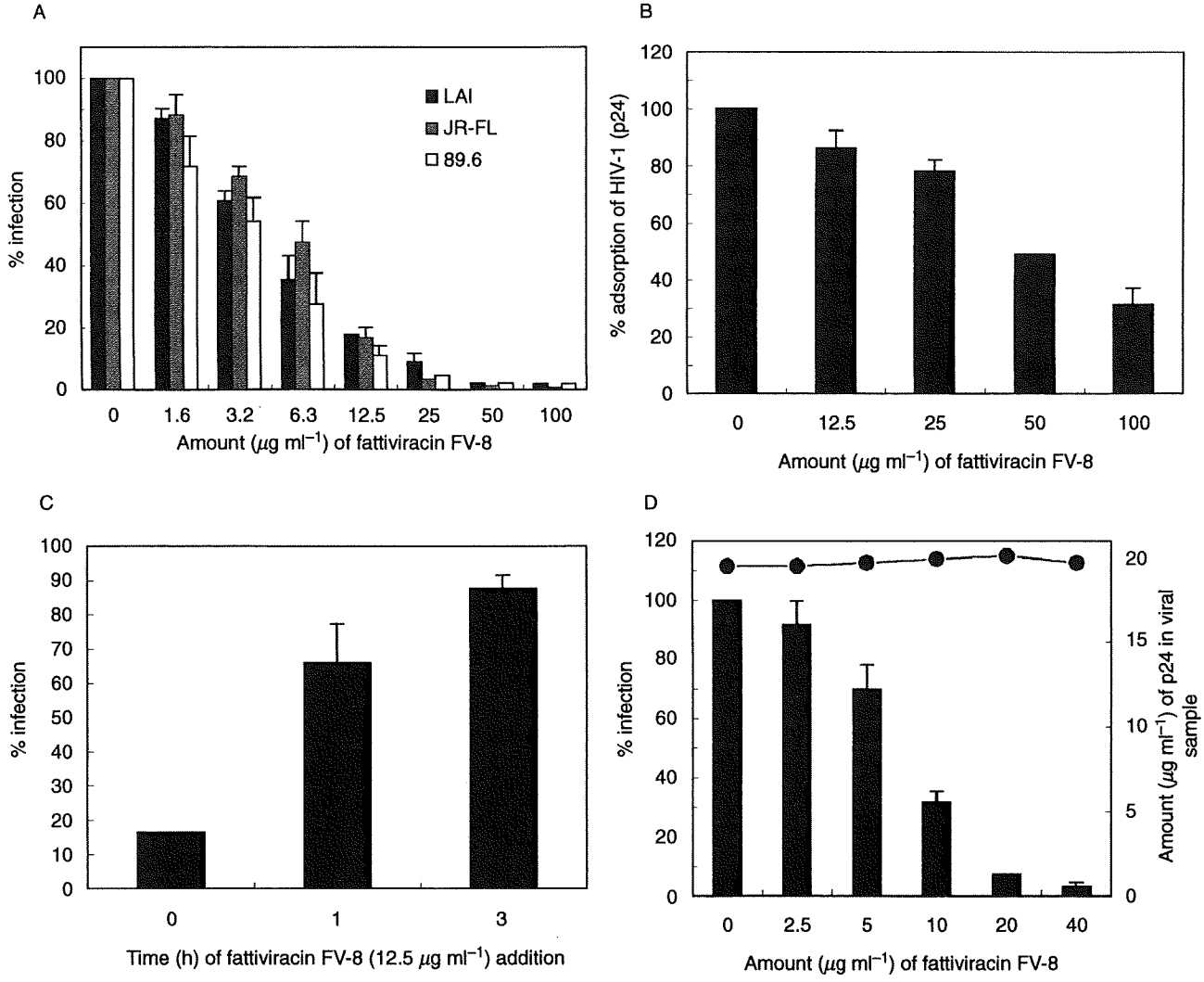

Fig. 1. Inhibitory effects of fattiviracin FV-8 on HIV-1 infection.
A. MAGI/CCR5 cells were infected with LAI, JR-FL and 89.6 viruses in the presence of serially diluted fattiviracin FV-8 in triplicate.
B. MAGI/CCR5 cells were incubated with LAI viruses at 37°C for 1 h in triplicate and washed twice with PBS. The amount of adsorbed viruses was assessed by p24 ELISA.
C. MAGI/CCR5 cells were infected with LAI viruses and fattiviracin FV-8 was added at 0, 1 and 3 h to obtain a final concentration of 12.5 μg ml^{-1}. The experiments were performed in triplicate.
D. LAI viruses in supernatants were treated with serially diluted fattiviracin FV-8. Each treated viral preparation after removing the excess glycolipid was subjected to determination of the p24 amount (line) and infectivity in triplicate (bar). Bars show the mean ± SD.

2001), fattiviracin FV-8 was most effective against HIV-1 infection when the compound was added during viral adsorption for 1 h, indicating that the glycolipid inhibited the early phase of the HIV-1 replication cycle after attachment. We further confirmed that direct treatment of X4 HIV-1 with serially diluted fattiviracin FV-8 for 1 h at 37°C reduced its infectivity dose-dependently and the EC_{50} was about 7.5 μg ml^{-1} (Fig. 1D). As the p24 amount of each viral preparation treated with fattiviracin FV-8 was unchanged at about 20 ng ml^{-1} (Fig. 1D), the glycolipid inhibited viral infection particularly not by lysing the viral particles.

Enhanced effects of fattiviracin FV-8 on HIV-1 infection by pretreatment of cells and effects on cell–cell fusion

The MAGI/CCR5 cells were treated with 200–800 μg ml^{-1} fattiviracin FV-8 for 1 h at 37°C and washed with medium. The glycolipid-pretreated cells were then infected with LAI, JR-FL and 89.6 strains of HIV-1 to assess their infectivity. Figure 2A shows that the infectivity of each virus increased six to eight times when the cells were pretreated with 600 μg ml^{-1} of fattiviracin FV-8. No significant effect was observed by the pretreatment with less than 50 μg ml^{-1}. The amount of adsorbed X4 viruses was

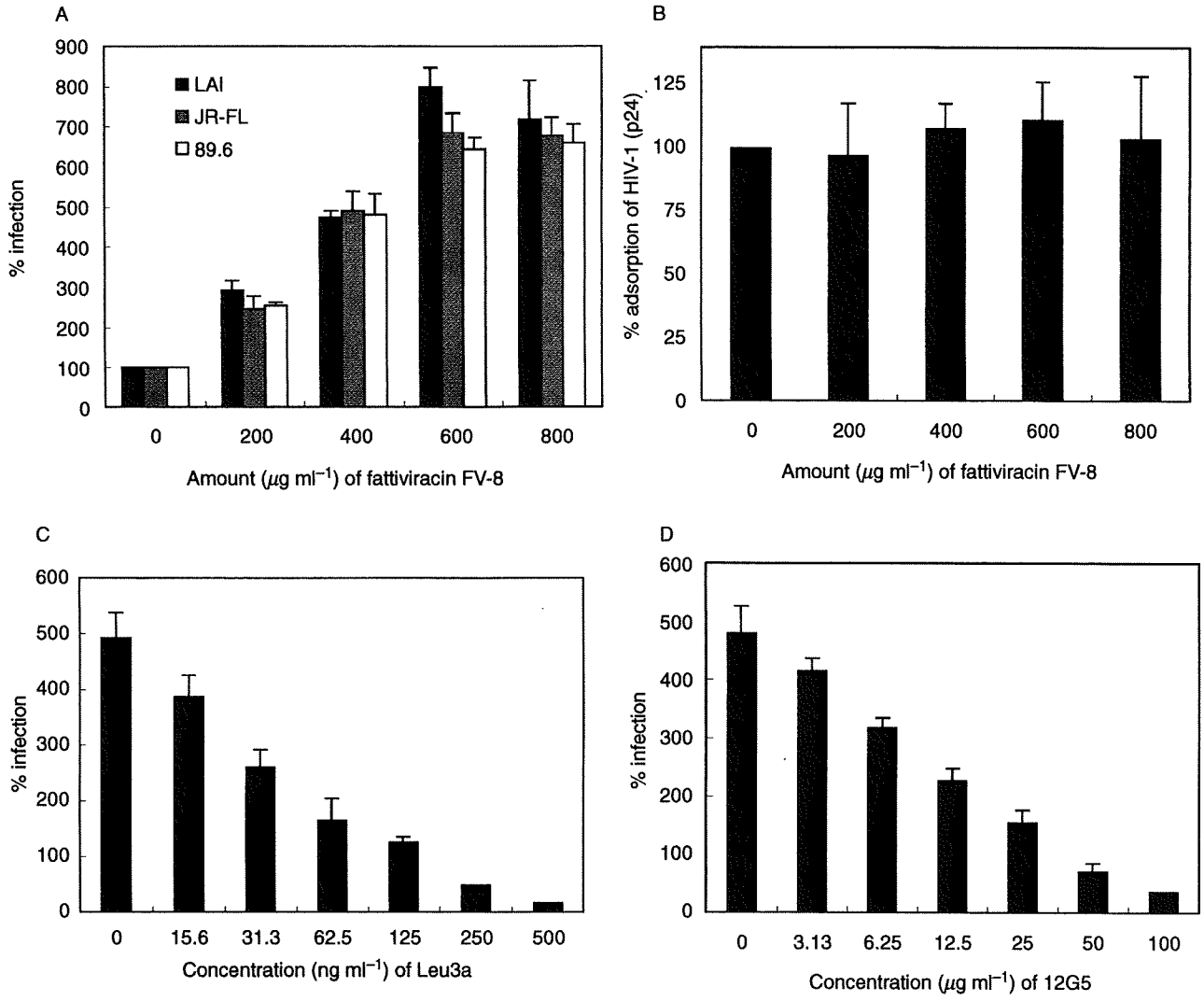

Fig. 2. Enhanced effects of fattiviracin FV-8 on HIV-1 infection.
A. MAGI/CCR5 cells were treated with serially diluted fattiviracin FV-8 at 37°C for 1 h and washed once with medium. Then, the pretreated cells were infected with LAI, JR-FL and 89.6 viruses in triplicate.
B. The fattiviracin FV-8-pretreated MAGI/CCR5 cells as in (A) were incubated with LAI viruses at 37°C for 1 h in triplicate and washed twice with PBS. The amount of adsorbed virus was assessed by p24 ELISA.
C. MAGI/CCR5 cells pretreated with 400 μg ml^{-1} fattiviracin FV-8 were infected with LAI viruses in the presence of serially diluted Leu 3a mAb in triplicate.
D. MAGI/CCR5 cells pretreated with 400 μg ml^{-1} fattiviracin FV-8 were infected with LAI viruses in the presence of serially diluted 12G5 mAb in triplicate. Bars show the mean ± SD.

not affected even though the cells were pretreated with 800 μg ml^{-1} of fattiviracin FV-8 (Fig. 2B). Fattiviracin FV-8 did not enhance the expression of CD4 nor CXCR4 by FACS analysis (data not shown). The enhanced infectivity of LAI HIV-1 by pretreatment of the cells is not a consequence of more viral adsorption (Fig. 2B), suggesting that the pretreatment of fattiviracin FV-8 may enhance the fusion step of viral entry. This enhancement was dose-dependently blocked by Leu 3a (Fig. 2C) and 12G5 (Fig. 2D) monoclonal antibodies, indicating that the increased infectivity was mediated by or depended on the amount of CD4 and CXCR4 molecules involved in fusion. The enhancement could result from accumulation of receptors at the site of viral attachment.

Next, the effect of fattiviracin FV-8 on cell–cell fusion was examined by coculturing chronically HIV-1 infected MOLT-4 (MOLT-4/HIV-1_{C-2}) cells with uninfected MOLT-4 cells (Fig. S1A) for 24 h. Fusion, which may relate to virological synapse (McDonald *et al.*, 2003), was completely inhibited by adding 20 μg ml^{-1} fattiviracin FV-8 to culture medium (Fig. S1B). When the MOLT-4/HIV-1_{C-2} cells were cocultured with target MOLT-4 cells pretreated

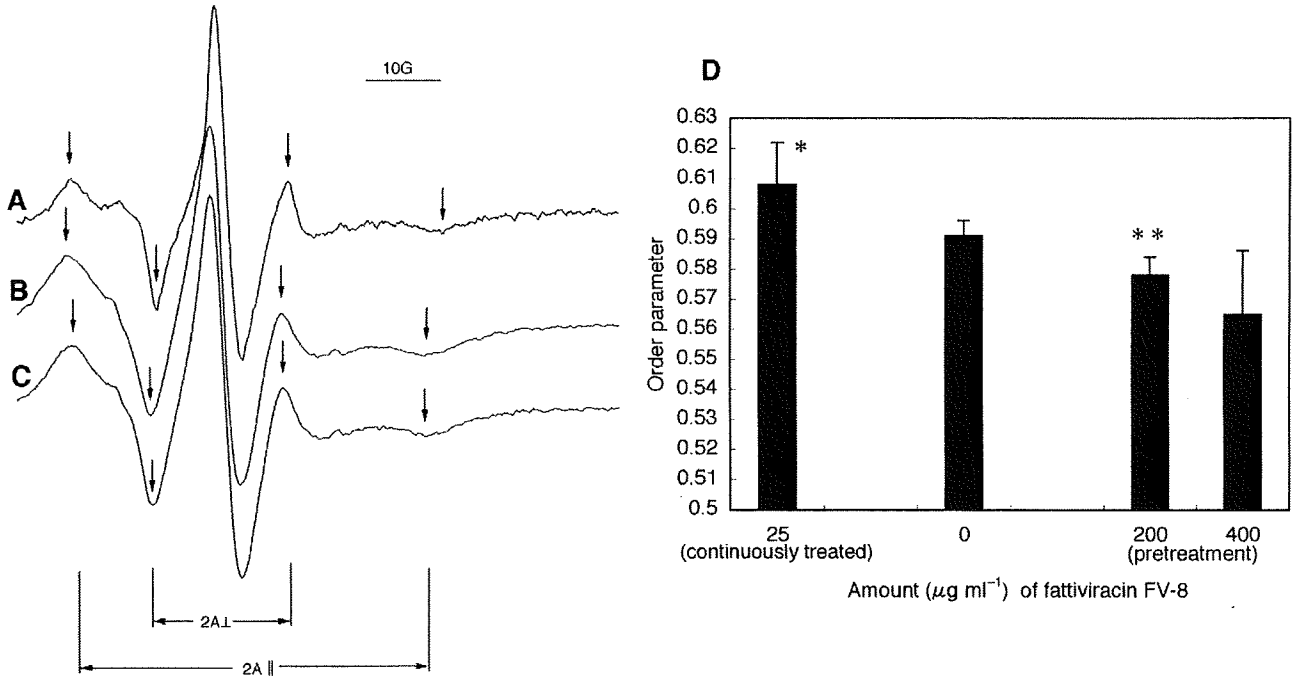

Fig. 3. Effects of fattiviracin FV-8 on the fluidity of the plasma membrane. ESR spectra of plasma membrane from MT-2 cells continuously treated with 25 μg ml^{-1} fattiviracin FV-8 (A), control MT-2 cells (B) and 200 μg ml^{-1} fattiviracin FV-8-pretreated MT-2 cells (C). The outer and inner hyperfine splitting, 2 $A_{//}$ and 2 $A_{\perp}$ were measured as shown by arrows. The scale of the horizontal axis (magnetic field) is shown as 10G. (D) MT-2 cells were treated with 25 μg ml^{-1} fattiviracin FV-8 and membrane fluidity was assessed in the presence of 25 μg ml^{-1} fattiviracin FV-8 (continuously treated, $n = 10$). MT-2 cells were pretreated with 200 and 400 μg ml^{-1} fattiviracin FV-8 and the fluidity was assessed in PBS (pretreatment, $n = 5$ each). Bars show the mean ± SD. *$P < 0.02$ compared with control (0 μg ml^{-1}) MT-2 cells ($n = 6$) and **$P < 0.01$ compared with control.

with 400 μg ml^{-1} fattiviracin FV-8, the glycolipid tended to enhance syncytium formation (Fig. S1C).

Effect of fattiviracin FV-8 on membrane fluidity

The electron spin resonance (ESR) spectra of MT-2 plasma membrane with 5-doxyl stearic acid (5-DSA) showed a typical pattern of anisotropic motion of the probe situated in the lipid bilayer (Fig. 3B). The ESR spectrum of MT-2 cells continuously treated with 25 μg ml^{-1} fattiviracin FV-8 showed a rather immobilized state (Fig. 3A), indicating that the motion of the 5-DSA spin probe was strongly restricted by the interaction with membrane constituents, probably incorporated fattiviracin FV-8 glycolipids. The order parameter was 0.608 ($n = 10$), significantly higher ($P < 0.02$) than that (0.591) of control MT-2 cells ($n = 6$) (Fig. 3D). When the cells were pretreated with 200 μg ml^{-1} fattiviracin FV-8, the ESR spectrum exhibited short $A_{//}$ (Fig. 3C) and the order parameter decreased to 0.578 ($n = 5$) (Fig. 3D), which was also significantly lower ($P < 0.01$) than the control MT-2 cells. When the cells were pretreated with 400 μg ml^{-1}, the order parameter tended to be lower than 200 μg ml^{-1}, but this was not significant due to undulation of the fluidity (Fig. 3D). Thus, fattiviracin FV-8 is a fluidity modulator, and the suppression and enhancement of membrane fluidity by the glycolipid were correlated with the decreased and increased susceptibility to HIV-1 infection and cell–cell fusion.

Theoretical mechanisms of antiviral activity and fluidity modulation by glycolipids

Both fattiviracin FV-8 and glycyrrhizin were fluidity modulators. Consequently, they showed similar effects on viral infection; first, the compounds were broad antiviral agents, especially against enveloped viruses; second, the compounds blocked cell–cell fusion induced by accumulation of cell-associated viral ligands and receptors; third, the compounds reduced the infectivity of virion itself when the viruses were pretreated; last, when cells were pretreated with high concentrations of the compounds, the cells exhibited enhanced susceptibility to viral infection and cell–cell fusion. All of the above effects can be explained by membrane fluidity modified by the compounds in terms of fusion-pore-formation due to accumulation of activated viral fusion peptides. A similar inhibitory effect of retrocyclin 2 on viral fusion and entry was reported, although retrocyclin 2 immobilized surface proteins by cross-linking membrane glycoproteins (Leikina

et al., 2005). Restricted movement of membrane molecules by cross-linking or decreased fluidity is actually critical to the entry of viruses, thus it can be applied to a new strategy to inhibit virus infection. As capsianoside G and fattiviracin FV-8 show similar potency (Table 1), both could be a potential candidate of broad antiviral agents.

Incorporation or exodus of movable macromolecules in or from the lipid-bilayer membrane produces dynamic changes in membrane fluidity, thus disturbing the lateral movement of proteins in the membrane. Amphipathic glycoproteins diffuse in and out the membrane through their hydrophilic and lipophilic domains. Diffusion efficiency may be determined by the amount of sugars, because longer sugar-chained molecules with more hydrophilic nature had less effect on HIV-1 infection (capsianoside G versus capsianoside A in Table 1). The presence of these molecules in the membrane may hamper the anisotropic movement of acyl chains of phospholipids. One can imagine that this 'diffusion and occupancy' may have a bearing on molecule movement in the membrane and in this manner influence viral entry, formation of synapses, and other membrane-mediated functions.

Experimental procedures

Cells and culture

MOLT-4, MOLT-4/HIV-1_{C-2} and MT-2 cells (Harada *et al.*, 1985) were cultured in RPMI1640 medium (Gibco BRL, Grand Island, NY) supplemented with 10% heat-inactivated fetal bovine serum (FBS), 2 mM L-glutamine, 100 IU ml^{-1} of penicillin and 0.1 mg ml^{-1} of streptomycin (complete medium). MAGI/CCR5 cells were cultured in Dulbecco minimal essential medium (ICN, Costa Mesa, CA) with 10% heat-inactivated FBS, 2 mM L-glutamine, 100 IU ml^{-1} penicillin, 0.1 mg ml^{-1} streptomycin, 0.1 mg ml^{-1} G418, 0.05 mg ml^{-1} hygromycin B and 0.05 mg ml^{-1} zeomycin as described (Song *et al.*, 2001).

Preparation of viruses

LAI (III_B) viruses (X4 HIV-1) were obtained from 3-day-old culture-supernatants of MOLT-4/HIV-1_{C-2} cells. JR-FL (R5 HIV-1) and 89.6 (X4R5 HIV-1) viruses were recovered by transfection of pJR-FL and p89.6, respectively, into COS-7 cells using Lipofectamine (Gibco) as described (Song *et al.*, 2001). The supernatants were filtered through 0.45 μm-pore-size filters and used as cell-free viruses.

Reagents

Sphingomyelin, sphingosine and lysophosphatidic acid were purchased from Sigma (St Louis, MO), dissolved at a concentration of 100 mg ml^{-1} in ethanol and stored at –20°C. The stock solution was diluted with phosphate-buffered saline (PBS) and sonicated for 10 min before use. Galactosylceramide (Galactocerebrosides from Sigma) and monosialoganglioside GM_1 (Sigma) were dissolved in ethanol at a concentration of 50 mg ml^{-1} and stored at –20°C. Capsianosides were extracted from *Capsicum annuum* and their structures were elucidated and reported elsewhere (Song *et al.*, 2001). Capsianosides were dissolved in methanol at 10 mg ml^{-1} and stored at –20°C until use. The volume of capsianosides required was dried in an eppendorf tube using a vacuum centrifugal concentrator, then dissolved in complete medium for each experiment. Fattiviracin FV-8 isolated from *Streptomycetes* was dissolved at a concentration of 50 mg ml^{-1} in PBS and stored at 4°C until use. 5-DSA was purchased from Sigma-Aldrich and stored at a concentration of 20 mg ml^{-1} in ethanol at 4°C. Anti-CD4 monoclonal antibody (mAb) Leu 3a and anti-CXCR4 mAb 12G5 were also purchased from Becton Dickinson (Lincoln Park, NJ) and R and D Systems (Minneapolis, MN) respectively.

Multinuclear activation of a galactosidase indicator assay

The MAGI/CCR5 cells (2×10^4 $well^{-1}$) that had been seeded the previous day on a flat 48 well plate were infected with LAI, JR-FL or 89.6 viruses. On day 2 post infection, infected MAGI/CCR5 cells were fixed with 1% formaldehyde and 2% glutaraldehyde in PBS for 5 min. Cells were then washed twice with PBS and incubated for 40 min at 37°C with staining solution (3 mM potassium ferrocyanide, 3 mM potassium ferricyanide, 1 mM $MgCl_2$ and 0.4 mg of Xgal in PBS). Blue nuclei were counted under a microscope (Kimpton and Emerman, 1992). Percentage infection was calculated as (% positive cells in test/% positive cells in control) × 100.

Adsorption of HIV-1

MAGI/CCR5 cells on a flat 48 well plate were incubated with 20 ng p24 of HIV-1 at 37°C for 1 h. The cells were washed twice with complete medium and lysed in 200 μl. The lysates were measured by p24 ELISA to assess the amount of adsorbed viruses. Percentage adsorption was calculated as (amount of p24 in test/amount of p24 in control) × 100.

Treatment of HIV-1 with fattiviracin FV-8

Viral supernatants were treated with serially diluted fattiviracin FV-8 at 37°C for 1 h and then ultracentrifuged at 100 000 *g* for 1 h at 4°C to obtain viral pellets. The pellets were resuspended with complete medium to remove the excess glycolipid and used to inoculate MAGI/CCR5 cells to assess infectivity. The resuspended viruses were also evaluated for the amount of p24 using ELISA.

Fusion assay

MOLT-4 and MOLT-4/HIV-1_{C-2} cells were used as target and effector cells, respectively, for the fusion assay. 0.5 ml (3×10^5) of MOLT-4 cells was mixed with the same amount of MOLT-4/HIV-1_{C-2} cells in the presence or absence of 20 μg ml^{-1} fattiviracin FV-8. In another experiment, MOLT-4 cells were treated with 400 μg ml^{-1} fattiviracin FV-8 at 37°C for 1 h and washed once

before mixing. The mixture (1 ml well^{-1}) was placed in a flat 24 well plate and cultured at 37°C for 24 h.

Measurement of membrane fluidity by ESR spectroscopy

One millilitre (7×10^6) of MT-2 cells was mixed with 1 ml of 60 μg ml^{-1} 5-DSA in PBS to give a final concentration of 30 μg ml^{-1}, and then incubated at 37°C for 20 min (Harada, 2005). The cells were washed 3 times with PBS to remove the free spin label. Pellets of cells were resuspended in 40 μl of PBS and drawn into a capillary tube, and the ends were sealed. The capillary tube was then placed into a quartz glass tube and taken from the P3 facility. Spectra were recorded at 37°C with a JES-RE1X ESR spectrometer (JEOL, Tokyo, Japan) equipped with a variable temperature control accessory. Instrument conditions were 2 min scan time, 5.0 mT sweep width, 0.1 mT field modulation width, 10 mW microwave power, and 0.3 s time constant. Figure 3 shows representative spectra, for which the outer hyperfine splitting indicates 2 $A_{//}$ and the inner one denotes 2 $A_{\perp}$: The horizontal axis reflects varying magnetic fields and the vertical axis represents absorption of microwaves. The order parameter (S) was calculated as follows; $S = (A_{//} - A_{\perp})/27.3G$.

P24 assay

The amount of HIV-1 core p24 was assessed by using HIV-1 p24 antigen ELISA (Cellular Products, Buffalo, NY) according to the manufacturer's protocol.

Statistical analysis

Statistical analyses were carried out using the Student's unpaired *t*-test, and a *P*-value of < 0.05 was statistically considered indicative of significance.

Acknowledgements

We thank W. Song and K. Nagao for their technical help and M. Uyeda and S. Yahara for supplying fattiviracin FV-8 and capsianosides respectively. The studies described in this manuscript were funded by the Ministry of Health, Labour and Welfare (Health Sciences Research Grants), and also supported in part by the Cooperative Research Project on Clinical and Epidemiological Studies of Emerging and Re-emerging Infectious Diseases (Renkei Jigyo: No. 78, Kumamoto University) of the Ministry of Education, Culture, Sports, Science, and Technology (Monbu-Kagakusho) of Japan.

References

Colman, P.M., and Lawrence, M.C. (2003) The structural biology of type I viral membrane fusion. *Nat Rev Mol Cell Biol* **4:** 309–319.

Gibbons, D.L., Erk, I., Reilly, B., Navaza, J., Kielian, M., Rey, F.A., and Lepault, J. (2003) Visualization of the target-membrane-inserted fusion protein of Semliki Forest virus by combined electron microscopy and crystallography. *Cell* **114:** 573–583.

Gibbons, D.L., Vaney, M., Roussel, A., Vigouroux, A., Reilly, B., Lepault, J., *et al.* (2004) Conformational change and protein–protein interactions of the fusion protein of Semliki Forest virus. *Nature* **427:** 320–325.

Habib, E.E., Yokomizo, K., Nagao, K., Harada, S., and Uyeda, M. (2001) Antiviral activity of fattiviracin FV-8 against human immunodeficiency virus type 1 (HIV-1). *Biosci Biotechnol Biochem* **65:** 683–685.

Harada, S. (2005) The broad anti-viral agent glycyrrhizin directly modulates the fluidity of plasma membrane and HIV-1 envelope. *Biochem J* **392:** 191–199.

Harada, S., Koyanagi, Y., and Yamamoto, N. (1985) Infection of HTLV-III/LAV in HTLV-I-carrying cells MT-2 and MT-4 and application in a plaque assay. *Science* **229:** 563–566.

Harada, S., Akaike, T., Yusa, K., and Maeda, Y. (2004a) Adsorption and infectivity of human immunodeficiency virus type 1 are modified by the fluidity of the plasma membrane for multiple-site binding. *Microbiol Immunol* **48:** 347–355.

Harada, S., Yusa, K., and Maeda, Y. (2004b) Heterogeneity of envelope molecules shown by different sensitivities to anti-V3 neutralizing antibody and CXCR4 antagonist regulates the formation of multiple-site binding of HIV-1. *Microbiol Immunol* **48:** 357–365.

Harada, S., Yusa, K., Monde, K., Akaike, T., and Maeda, Y. (2005) Influence of membrane fluidity on human immunodeficiency virus type 1 entry. *Biochem Biophys Res Commun* **329:** 480–486.

Kimpton, J., and Emerman, M. (1992) Detection of replication-competent and pseudotyped human immunodeficiency virus with a sensitive cell line on the basis of activation of an integrated β-galactosidase gene. *J Virol* **66:** 2232–2239.

Leikina, E., Delanoe-Ayari, H., Melikov, K., Cho, M., Chen, A., Waring, A.J., *et al.* (2005) Carbohydrate-binding molecules inhibit viral fusion and entry by crosslinking membrane glycoproteins. *Nat Immunol* **6:** 995–1001.

McDonald, D., Wu, L., Bohks, S.M., Kewal Ramani, V.N., Unutmaz, D., and Hope, T.J. (2003) Recruitment of HIV and its receptors to dendritic cell-T cell junctions. *Science* **300:** 1295–1297.

Modis, Y., Ogata, S., Clements, D., and Harrison, S.C. (2004) Structure of the dengue virus envelope protein after membrane fusion. *Nature* **427:** 313–319.

Plonsky, I., and Zimmerberg, J. (1996) The initial fusion pore induced by baculovirus gp64 is large and forms quickly. *J Cell Biol* **135:** 1831–1839.

Roche, S., and Gaudin, Y. (2002) Characterization of the equilibrium between the native and fusion-inactive conformation of rabies virus glycoprotein indicates that the fusion complex is made of several trimers. *Virology* **297:** 128–135.

Song, W., Yahara, S., Maeda, Y., Yusa, K., Tanaka, Y., and Harada, S. (2001) Enhanced infection of an X4 strain of HIV-1 due to capping and colocalization of CD4 and CXCR4 induced by capsianoside G, a diterpene glycoside. *Biochem Biophys Res Commun* **283:** 423–429.

Tsunakawa, M., Komiyama, N., Tenmyo, O., Tomita, K., Kawano, K., Kotake, C., *et al.* (1992a) New antiviral antibiotics, cycloviracins B_1 and B_2 I. Production, isolation, physico-chemical properties and biological activity. *J Antibiot* **45:** 1467–1471.

Tsunakawa, M., Kotake, C., Yamasaki, T., Moriyama, T., Konishi, M., and Oki, T. (1992b) New antiviral antibiotics, cycloviracins B_1 and B_2 I. Structure determination. *J Antibiot* **45:** 1472–1480.

Uyeda, M., Yokomizo, K., Miyamoto, Y., and Habib, E.E. (1998) Fattiviracin A1, a novel antiherpetic agent produced by streptomyces microflavus strain, 2445, I. Taxonomy, fermentation, isolation, physico-chemical properties and structure elucidation. *J Antibiot* **51:** 823–828.

Yokomizo, K., Miyamoto, Y., Nagao, K., Kumagae, E., Habib, E.E., Suzuki, K., *et al.* (1998) Fattiviracin A1, a novel antiherpetic agent produced by streptomyces microflavus strain, 2445, II. Biological properties. *J Antibiot* **51:** 1035–1039.

Supplementary material

The following supplementary material is available for this article online:

Fig. S1. Effects of fattiviracin FV-8 on cell–cell fusion. MOLT-4 cells were cocultured with MOLT-4/HIV-$1_{C\text{-}2}$ cells in the absence (A) or presence (B) of 20 μg ml^{-1} fattiviracin FV-8. MOLT-4 cells pretreated with 400 μg ml^{-1} fattiviracin FV-8 were cocultured with MOLT-4/HIV-$1_{C\text{-}2}$ cells (C). Bar, 100 μm.

This material is available as part of the online article from http://www.blackwell-synergy.com

Impact of Intrinsic Cooperative Thermodynamics of Peptide-MHC Complexes on Antiviral Activity of HIV-Specific CTL[1]

Chihiro Motozono,* Saeko Yanaka,† Kouhei Tsumoto,† Masafumi Takiguchi,* and Takamasa Ueno[2]*

The antiviral activity of HIV-specific CTL is not equally potent but rather is dependent on their specificity. But what characteristic of targeted peptides influences CTL antiviral activity remains elusive. We addressed this issue based on HLA-B35-restricted CTLs specific for two overlapping immunodominant Nef epitopes, VY8 (VPLRPMTY) and RY11 (RPQVPLRPMTY). VY8-specific CTLs were more potently cytotoxic toward HIV-infected primary CD4$^+$ cells than RY11-specific CTLs. Reconstruction of their TCR revealed no substantial difference in their functional avidity toward cognate Ags. Instead, the decay analysis of the peptide-MHC complex (pMHC) revealed that the VY8/HLA-B35 complex could maintain its capacity to sensitize T cells much longer than its RY11 counterpart. Corroboratively, the introduction of a mutation in the epitopes that substantially delayed pMHC decay rendered Nef-expressing target cells more susceptible to CTL killing. Moreover, by using differential scanning calorimetry and circular dichroism analyses, we found that the susceptible pMHC ligands for CTL killing showed interdependent and cooperative, rather than separate or sequential, transitions within their heterotrimer components under the thermally induced unfolding process. Collectively, our results highlight the significant effects of intrinsic peptide factors that support cooperative thermodynamics within pMHC on the efficient CTL killing of HIV-infected cells, thus providing us better insight into vaccine design. *The Journal of Immunology,* **2009, 182: 5528–5536.**

Human CD8$^+$ CTLs recognize HIV-infected cells by interaction of their own TCRs with viral peptides bound to HLA class I molecules on the cell surface of the infected cells and eliminate them directly by cytolysis or indirectly through the production of soluble factors such as cytokines and chemokines. Among these activities, the cytotoxic activity of CTLs toward HIV-infected cells is associated with efficient viral containment in vitro and in vivo (1–3). However, significant differences exist not only in the antiviral activity of HIV-specific CTLs among specificities (4–7) but also in CTL specificities between early and chronic phases of an HIV infection (8–10). Changes in CTL specificity could lead to the accumulation of less effective antiviral CTLs in the late chronic phase of an infection (6, 11, 12). There are a number of different possibilities in the literature that potentially explain the heterogeneity in the antiviral activity of CTLs, such as: differences in functional avidity of CTLs toward exogenously pulsed synthetic peptides (7, 13), TCR usage (14, 15), cross-reactive capacity of CTLs toward variant Ags (14, 16), kinetics and amplitude of immunogenic protein expression (9, 17–19), Ag processing and presentation pathways (20, 21), and binding activity of an antigenic peptide to a given HLA class I molecule (22). However, considering that immunodominant peptides are not always those with the highest density presented at the target cell surface (23, 24) and that immunodominant CTLs are not always correlated with effective antiviral CTL responses (25), an interesting question can be raised as to whether, and if so what, inherent characteristics of target epitope peptides support the efficient recognition by CTLs for the killing of virus-infected cells. As mentioned above, however, the antiviral activity of CTLs stems from multifactorial events, reflecting the consequence of various positive and negative factors that govern viral replication, Ag presentation, and T cell activation (26). Broad comparisons between very different virus strains, peptide Ags, and MHCs provide little information beyond highlighting just the differences. Comparisons between more closely related viral Ags and MHCs could be more revealing.

We previously reported that CD8 T cells specific for an Nef epitope (VY8, VPLRPMTY) were consistently elicited very early in vivo, whereas those specific for another Nef epitope (RY11, RPQVPLRPMTY) were mostly observed in the chronic phase of an HIV infection (10). Remarkably, VY8 is entirely contained within RY11; and both are presented by HLA-B35 with comparable binding activity, as assessed by a cellular HLA stabilization assay (10). As initial preliminary experiments showed that VY8-specific CTLs had more potent cytotoxic activity toward HIV-infected primary CD4$^+$ cells than RY11-specific CTLs, in the present study we asked what property of these antigenic peptides is correlated with CTLs having potent antiviral cytotoxic activity. Combining a series of data obtained from T cell lines transduced with the genes for the cognate TCRs, we discovered that the decay of peptide-MHC class I complex (pMHC),[3] rather than the functional avidity of TCR-pMHC interactions, substantially influenced the susceptibility of HIV-infected cells to CTL

*Division of Viral Immunology, Center for AIDS Research, Kumamoto University, Kumamoto, Japan, and †Department of Medical Genome Sciences, Graduate School of Frontier Sciences, The University of Tokyo, Kashiwa, Japan

Received for publication October 15, 2008. Accepted for publication February 25, 2009.

The costs of publication of this article were defrayed in part by the payment of page charges. This article must therefore be hereby marked *advertisement* in accordance with 18 U.S.C. Section 1734 solely to indicate this fact.

[1] This research was supported in part by a grant-in-aid for scientific research from the Ministry of Education, Science, Sports, and Culture of Japan (to T.U.), by a grant from Human Science Foundation (to T.U.), and by a grant-in-aid for AIDS research from the Ministry of Health, Labor, and Welfare of Japan (to T.U. and M.T.).

[2] Address correspondence and reprint requests to Dr. Takamasa Ueno, Division of Viral Immunology, Center for AIDS Research, Kumamoto University, 2-2-1 Honjo, Kumamoto, 860-0811, Japan. E-mail address: uenotaka@kumamoto-u.ac.jp

[3] Abbreviations used in this paper: pMHC, peptide-MHC class I complex; DSC, differential scanning calorimetry; CD, circular dichroism; β_2m, β_2-microglobulin.

www.jimmunol.org/cgi/doi/10.4049/jimmunol.0803471

killing. Furthermore, by using a biochemical approach, we found that the peptide intrinsic cooperative thermodynamics of pMHC could be an important factor to support efficient antiviral cytotoxic activity of CTLs.

Materials and Methods

Generation of CTL clones and analysis of TCR-encoding genes

CTL clones were established as previously described (6, 15) by using PBMC samples taken from *HLA-B*3501*$^+$ individuals (Pt-01, Pt-03, Pt-19, and Pt-33) in the chronic phase of an HIV-1 infection. Briefly, a bulk CTL culture, which had been established by stimulation of PBMC with a synthetic peptide for 1–2 wk, was further seeded at a density of 0.8 or 5 cells/well with a cloning mixture (irradiated allogeneic PBMC and C1R-B3501 cells pulsed with 1 μM peptide in RPMI 1640 with 10% FCS and 100 U/ml recombinant IL-2). Two weeks later, cells showing substantial Ag-specific cytolytic activity were maintained in the medium with peptide stimulation weekly. CTL clone 139 generated from PBMC of Pt-19 was designated as CTL 19-139, and other clones were similarly designated. TCR-encoding genes of CTL clones were obtained by using a SMART PCR cDNA synthesis kit (BD Clontech) and analyzed by the ImMunoGeneTics database (http://imgt.cines.fr) as previously described (27, 28). The study was conducted in accordance with the human experimentation guidelines of Kumamoto University.

Reconstruction of TCRs on TCR-deficient T cells

The cDNAs encoding full-length TCRα and TCRβ of interest were separately cloned into a retrovirus vector pMX provided by T. Kitamura (Tokyo University, Tokyo, Japan) and delivered into a TCR-deficient mouse T cell hybridoma cell line TG40 provided by T. Saito (RIKEN Institute, Saitama, Japan) as previously described (27, 28). The human CD8α gene was similarly delivered into the cells as needed (28). Finally the cells showing bright staining with PE-conjugated anti-mouse CD3ε mAb (2C11; BD Pharmingen) were cloned by a limiting dilution method for further functional assays described below.

HLA-B35 tetramer binding assays

The HLA-B*3501 tetramers in complex with the VY8 or RY11 peptides were prepared as previously described (28). The CTL clones were stained with PE- and allophycocyanin-labeled HLA-B35 tetramers at 37°C for 15 min followed by anti-CD8-PerCP (BD Biosciences) and anti-CD3-FITC (DakoCytomation) at 4°C for 15 min. For the kinetic analysis of HLA-B35 tetramer dissociation, CTL clones were stained with PE-conjugated tetramer (0.2 μM) for 30 min at 4°C. Then the cells were rapidly washed twice and suspended at 4°C in a buffer (2% BSA in PBS) supplemented with the monomeric type of unconjugated peptide-HLA complex (2 μM) for blocking. A portion of the reaction volume was then removed periodically (0.5, 1, 2, 4, and 8 h), and the cells were subsequently stained with anti-CD8 and anti-CD3 mAbs at 4°C. For the flow cytometric analysis, the CD3$^+$CD8$^+$ cells were gated and then analyzed for the tetramer binding by flow cytometry with FACSCalibur (BD Biosciences).

Cytotoxicity assays

Primary CD4$^+$ cells were purified from PBMC taken freshly from HIV-negative donors expressing *HLA-B*3501* by using a magnetic cell separation system (Miltenyi Biotec) and stimulated with PHA (3 μg/ml; Sigma-Aldrich) for 4 days. After having been labeled with ^{51}Cr, the activated CD4$^+$ cells were pulsed with various concentrations of a synthetic peptide for 1 h at 37°C, washed once with culture medium, and then mixed with CTL clones (4000 cells/well) for 4 h at 37°C. For virus-infected target cells, the activated CD4$^+$ cells (4000 cells/well), which had been infected with recombinant HIV-1 or vaccinia virus carrying the *nef* gene of strain SF2 (10), were mixed with CTL clones at various E:T ratios for 6 h at 37°C after having been labeled with ^{51}Cr. It should be noted that 30 ± 5% of the cells were p24 Ag-positive, as revealed by intracellular flow cytometric analysis of HIV-infected CD4$^+$ cells.

IL-2 assays for T cell activation

TCR recognition of cognate Ags was measured in terms of IL-2 secretion by TG40 cells transduced with TCR and CD8α as described earlier (27, 28). Unless otherwise specified, C1R-B3501 cells (10^4 cells/well), TCR-transduced TG40 cells (2×10^4 cells/well), and peptides were mixed and incubated for 48 h at 37°C. The resultant culture supernatant was then collected, and the amount of IL-2 was determined by analyzing the proliferative activity of CTLL-2, an IL-2 indicator cell line. The EC_{50} value of the peptide was calculated as the concentration of peptide that exhibited a half-maximal activation of TCR-transduced TG40 cells with CD3ε mAb-mediated activation of the cells defined as maximal.

pMHC decay assay

For the kinetic analysis of the peptide dissociation from pMHC, C1R-B3501 cells were first incubated with 100 μM peptide at 37°C for 1 h. Then the cells were rapidly washed twice and suspended at 37°C in culture medium. A portion of the peptide-loaded target cells was then removed periodically (10, 20, 30, 60, 120, 240, 360, 720 min), washed once with culture medium, and subsequently mixed with TCR-transduced TG40 cells. The amount of IL-2 produced by the TG40 cells was then determined as described.

Differential scanning calorimetry (DSC) and circular dichroism (CD) analyses

The extracellular domain of HLA-B*3501 H chain (aa residues 1–276) and β_2-microglobulin (β_2m) were produced in *Escherichia coli* as insoluble inclusion bodies. These proteins were dissolved in a buffer containing urea and then refolded in the presence of synthetic VY8 or RY11 peptide as previously described (28). In this construct, there was no biotinylated tag sequence at the C terminus of the H chain. Refolded proteins were purified by size-exclusion and anion-exchange chromatography analysis, pooled, dialyzed against PBS (137 mM NaCl, 2.7 mM KCl, 10 mM Na_2HPO_4, 1.8 mM KH_2PO_4 (pH 7.5)), and used both for DSC and CD measurements. The resultant protein solutions were in the concentration range from 0.3 to 0.7 mg/ml, as determined by UV absorption at 280 nm; and the molecular masses of the protein complexes were calculated from the amino acid composition.

For DSC measurements, excessive heat capacity curves were monitored by an ultrasensitive scanning microcalorimeter (VP-DSC; MicroCal) at a heating rate of 1 K/min with a sample cell volume of ~0.5 ml. The experimental data were baseline-corrected and subjected to deconvolution by using the software package ORIGIN for DSC (MicroCal), based on the assumption that the macromolecule is composed of a number of domains, each of which is involved independently in a "two-state" transition between folded and unfolded states. Each transition is characterized by two parameters, T_m and ΔH_m, in which T_m is the thermal midpoint of a transition and ΔH_m is the calorimetric heat change calculated from the area under the transition peak.

For CD measurements, changes in the ellipticity (as θ) with heating from 4° to 90°C were monitored at 222 nm and other wavelengths by a JASCO J-725 spectropolarimeter with a sample cell volume of ~0.4 ml in a quartz cell with an optical path length of 2 mm. The T_m value in the CD analysis was calculated by using the standard analysis software provided by the manufacturer (JASCO).

Results

Antiviral cytotoxic activity of CTLs specific for VY8 or RY11

We previously reported that in HIV-infected patients with *HLA-B35*, Nef protein elicited the most dominant CD8 T cell responses (6), with a short epitope (VY8, VPLRPMTY) being dominant early and a subsequent shift to an N-terminal extended long epitope (RY11, RPQVPLRPMTY) in the chronic phase (10). However, VY8 is entirely contained within RY11 and may therefore be the minimum epitope for CTLs. To clarify this issue, we generated CTL clones by stimulating PBMC of four HIV-infected individuals with either VY8 or RY11 peptide and then analyzed their Ag fine specificity by cytotoxic assays. Three CTL clones (01-127, 19-139, and 33-1) generated with VY8 stimulation showed a potent cytotoxic activity toward primary CD4$^+$ cells pulsed with VY8 and an activity of markedly lesser strength toward those pulsed with RY11 peptide (Fig. 1*A*), confirming their optimal epitope to be VY8. In contrast, the other three CTL clones (01-113, 01-231, and 03-8) generated with RY11 stimulation showed a potent cytotoxic activity toward primary CD4$^+$ cells pulsed with RY11 and no activity toward those pulsed with VY8 (Fig. 1*A*), confirming their optimal epitope to be RY11. Ag fine specificity of the CTL clones was also confirmed in terms of the HLA-B35 tetramer binding (see below). These data indicate that

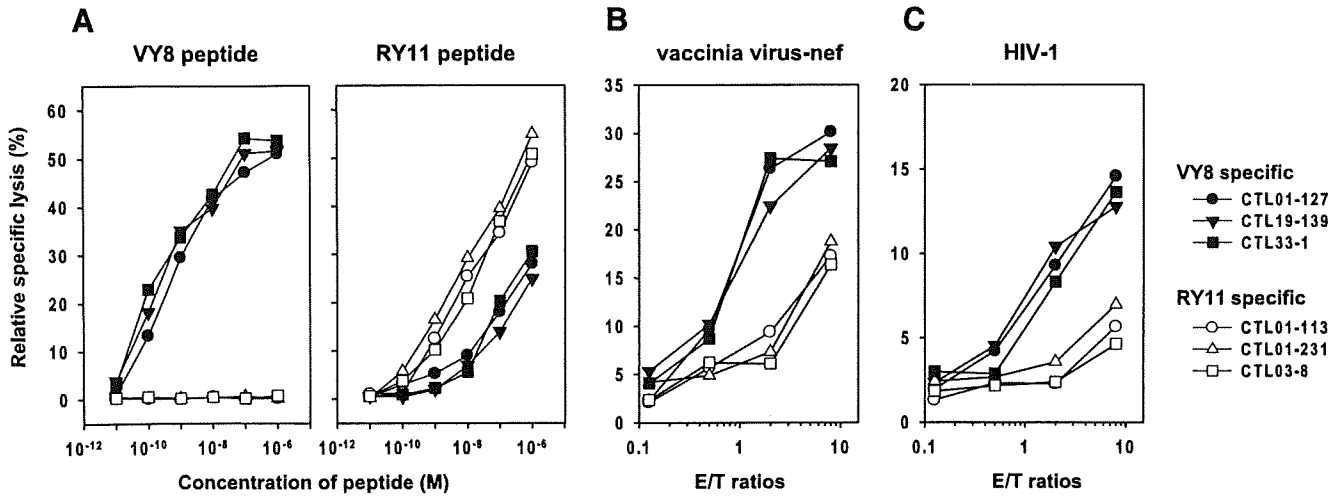

FIGURE 1. Cytotoxic activity of CTL clones. Primary $CD4^+$ cells isolated from an HIV-negative donor were pulsed with various concentrations of VY8 or RY11 peptide (*A*), infected with recombinant vaccinia virus expressing Nef_{SF2} (*B*), or infected with HIV-1 (*C*) and then mixed with the indicated CTL clones. To obtain relative specific lysis values, the cytotoxic activity toward the same target cells not pulsed with peptide, infected with vaccinia virus alone (i.e., lacking *nef* expression) or infected with HIV-1 Δ*nef* variant was determined in parallel and was deducted as a background value. Data presented are the mean of duplicate assays, and an additional set of experiments using another PBMC donor showed similar results.

VY8 and RY11 are optimal epitopes for HLA-B35 and are recognized by a different set of CTL clones.

We next asked whether CTL antiviral cytotoxic activity is different between specificities. The CTL clones showed a significant difference in functional avidity toward their cognate Ags between the specificities ($p = 0.023$, two-tailed t test), with EC_{50} values being $2.9 \pm 0.85 \times 10^{-10}$ and $1.3 \pm 0.37 \times 10^{-8}$ M for VY8 and RY11, respectively (Fig. 1*A*). Next, the same cells were infected with vaccinia virus or HIV-1 expressing Nef_{SF2} and analyzed for their susceptibility to killing by the CTL clones. The VY8-specific CTLs showed more potent cytotoxic activity toward virus-infected $CD4^+$ cells than the RY11-specific ones regardless of the viruses used (Fig. 1, *B* and *C*).

Kinetics of interactions between CTLs and HLA tetramers

We next examined TCR-pMHC interactions by analyzing the binding specificity and activity of CTL clones toward HLA-B35 tetramers. CTL 19-139 and 01-231 were exclusively stained by their cognate HLA-B35 tetramers, whereas an Env-specific CTL clone was not stained by any of the HLA-B35 tetramers examined (Fig. 2*A*), confirming the specificity of the CTL clones as well as the integrity of our peptide-HLA class I complex preparations. Also, titration of the HLA-B35 tetramers showed comparable binding activity of the CTL clones toward the cognate HLA-B35 tetramers (Fig. 2*B*). We then examined the kinetics of the dissociation of cognate HLA-B35 tetramers from CTL clones. There was no substantial difference between CTL 19-139 and CTL 01-231 in dwell time of interaction with the cognate HLA-B35 tetramers (Fig. 2*C*), suggesting comparable kinetic interactions between VY8 and RY11-specific TCRs and their cognate pMHC. However, these results appeared to be inconsistent with the data showing the favorable functional avidity of VY8-specific CTLs (as described).

Functional reconstruction of TCRs on TCR-deficient T cells

It has been shown that TCR reconstruction on TCR-deficient T cells is advantageous to investigate how the TCR-pMHC interaction influences T cell activation (27–30) because primary T cells can increase or decrease their sensitivity/avidity for an epitope through changes in their inhibitory receptor expression and membrane organization as well as via a redistribution of signaling molecules in

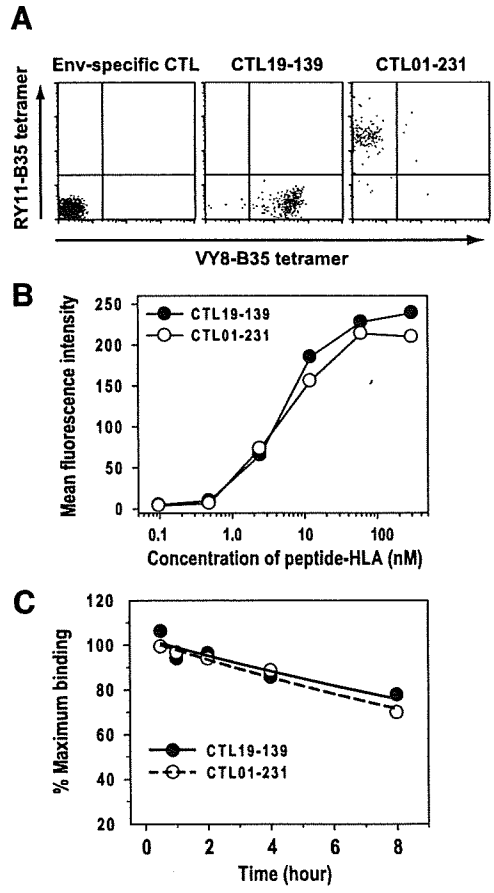

FIGURE 2. HLA tetramer analysis of CTL clones. *A*, CTL clones specific for an Env peptide, VY8 (CTL 19-139) or RY11 (CTL 01-231), were stained with HLA-B35 tetramers in complex with VY8 or RY11 that had been labeled with PE or allophycocyanin, respectively. In the flow cytometric analysis, a live $CD8^+$ subset was gated and analyzed for binding with HLA-B35 tetramers. *B*, CTL 19-139 and CTL 01-231 were separately stained with various concentrations of PE-conjugated HLA-B35 tetramers in complex with their cognate peptides and analyzed by flow cytometry. An independent experiment gave similar results. *C*, Kinetic analysis of dissociation of HLA-B35 tetramers from CTL 19-139 and CTL 01-231 that had been stained with their cognate HLA-B35 tetramers. An independent experiment gave similar results.

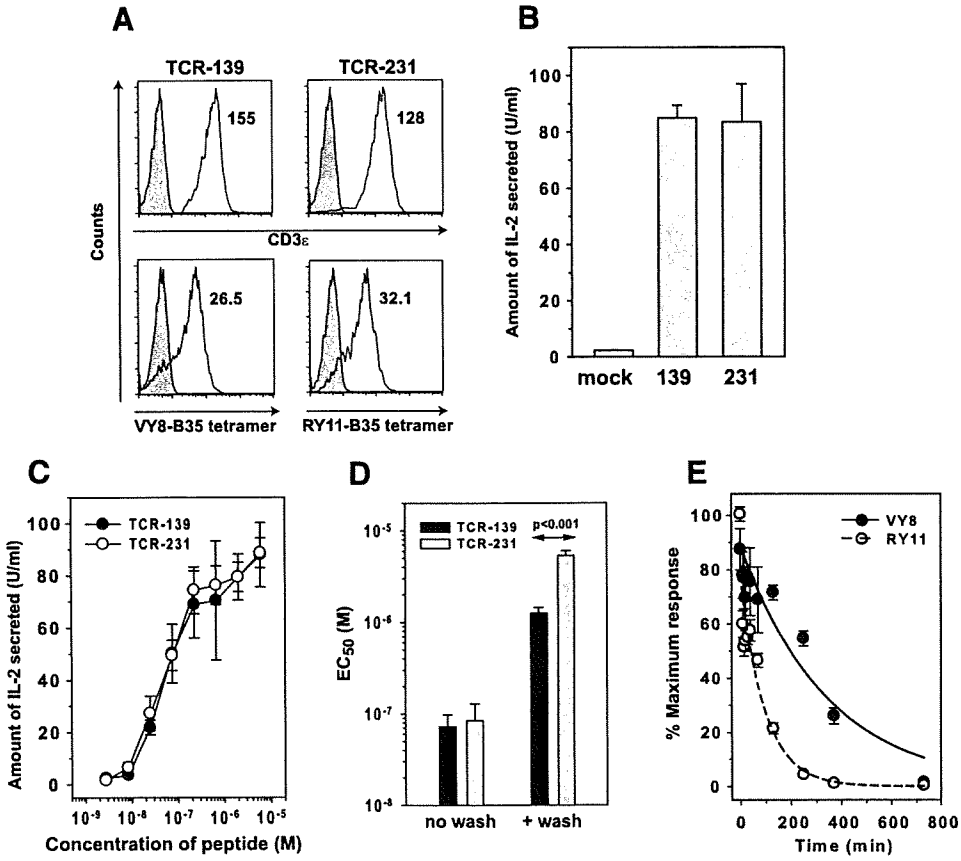

FIGURE 3. TCR-pMHC interactions on TCR-transduced TG40 cells. *A*, TG40 cells alone (shaded histogram) or those expressing TCR-139 or TCR-231 (open histogram) were stained with anti-CD3ε mAb and their cognate HLA-B35 tetramers and then analyzed by flow cytometry. The mean fluorescence intensity is indicated in each histogram. *B*, IL-2 secretion of TG40 cells transduced with mock, TCR-139 or TCR-231 in response to stimulation with CD3ε mAb. Data are the mean ± SD of quadruplicate assays. *C*, IL-2 secretion by TG40 cells transduced with TCR-139 or TCR-231 in response to various concentrations of VY8 or RY11, respectively. TG40 cells, C1R-B3501 cells, and the peptide were coincubated for the duration of the assay. The amount of IL-2 obtained for the mock-transduced TG40 cells was always <5.0. Data are the mean ± SD of quadruplicate assays. *D*, Functional avidity of TG40-139 and TG40-231 cells were dependent of assay conditions. C1R-B3501 cells, the peptide, and TG40 cells were coincubated for the duration of the assay (no wash). C1R-B3501 cells and the peptide were incubated, washed, and subsequently mixed with the TG40-139 or TG40-231 cells (with wash). The EC_{50} values (mean ± SD) were obtained from quadruplicate assays. Statistical analysis was performed using the two-tailed *t* test. *E*, Kinetic analysis of the peptide dissociation from pMHC. C1R-B3501 cells were pulsed with the VY8 or RY11 peptide (100 μM) and washed. A portion of the resultant peptide-loaded cells was taken at each indicated time point and then mixed with TG40-139 or TG40-231 cells for the IL-2 secretion assay. Results are mean ± SD of triplicate assays expressed relative to the maximum response that was arbitrarily set to 100%. The lines shown are based on a single exponential decay.

some circumstances (31–35). To further clarify how the TCR-pMHC interacts, we cloned TCR-encoding genes of CTL 19-139 (VY8 specific) and CTL 01-231 (RY11 specific), and functionally reconstructed their TCRs (designated TCR-139 and TCR-231, respectively) on TCR-deficient T cell line TG40 (27, 28). The resultant TG40-139 and TG40-231 cells showed CD3 expression and HLA-B35 tetramer binding activity at comparable levels (Fig. 3*A*), in good agreement with the observations obtained for the parental CTLs (Fig. 2, *B* and *C*). After further transduction of the cells with human CD8α, both cells showed IL-2 secretion at a comparable level in response to anti-CD3 mAb stimulation (Fig. 3*B*), confirming the integrity of the TCR-mediated signaling machinery in these cells. Then, functional avidity of TG40-139 and TG40-231 cells toward the cognate Ags was determined by coincubation of target cells and peptides. Virtually no difference was observed in their functional avidities (Fig. 3*C*), suggesting comparable TCR-pMHC interactions between the specificities. It should be noted that the peptides were always present for the duration of the assay (see below).

Effect of peptide-off rate on functional avidity of T cells

During a number of attempts to clarify the reasons for the variable observations among assays, we noticed that the avidity of TCR-transduced cells was much decreased when the peptide-loaded target cells were washed before coincubation with the TCR-transduced cells (Fig. 3*D*). Under this washing-off condition, TG40-139 cells showed significantly more potent functional avidity than TG40-231 cells (Fig. 3*D*). We then analyzed the rate of peptide-off from pMHC by using the TCR-transduced cells. The target cells, which had been loaded with a peptide followed by washed-off, were taken and subsequently mixed with TG40 cells expressing the cognate TCR. The extent of the TG40 response should be proportional to the actual pMHC dose retained on the target cell surface. The data showed that the decay of the VY8/HLA-B35 complex was much slower than that of the RY11/HLA-B35 one, as the half-life values of pMHC were $3.3 \pm 0.83 \times 10^2$ and $1.0 \pm 0.03 \times 10^2$ min for VY8 and RY11, respectively (Fig. 3*E*).

Effects of antigenic variations on pMHC decay

To look for variant peptides that could affect pMHC decay and the susceptibility to stimulation of T cells, we examined a series of alanine substitutions in both peptides for their activity to sensitize TCR-transduced T cells under the no-wash condition. VY8 with an alanine substitution at position 5 (designated VY8-5A) showed

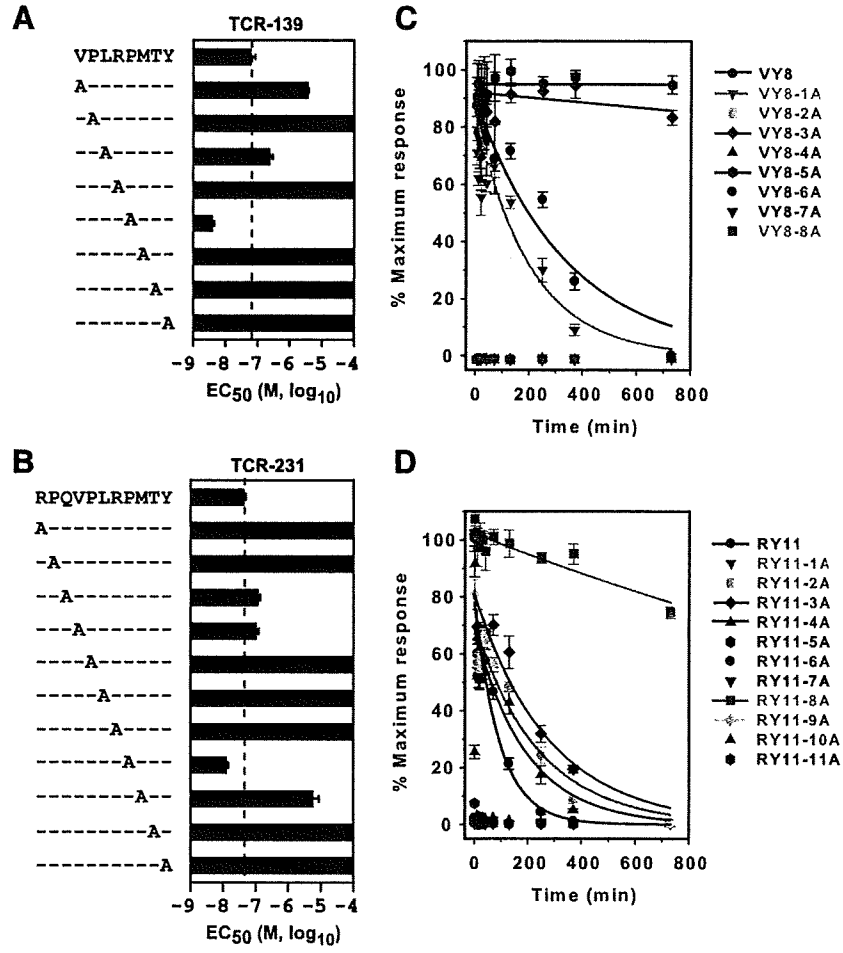

FIGURE 4. Effects of antigenic variations on pMHC decay. *A* and *B*, Alanine variants of VY8 and RY11 were examined by conducting T cell sensitization assays for TCR-139 (*A*) and TCR-231 (*B*), respectively. Amounts of IL-2 secreted by TG40 cells were determined under the no-wash condition. The maximum concentration of the peptides tested was 100 μM. The EC_{50} values at mean ± SD were obtained by performing triplicate assays. An independent experiment gave similar results. *C* and *D*, Dissociation of the wild-type and the alanine variants for VY8 (*C*) and RY11 (*D*) from pMHC was analyzed as in Fig. 3*E*. Data are mean ± SD of triplicate assays. An independent experiment gave similar results. The lines are based on a single exponential decay and given only for the peptides showing positive responses.

more potent reactivity with TCR-139 than did VY8, whereas VY8-1A and VY8-3A had moderate reactivity (Fig. 4*A*). However, TG40-139 cells did not respond to the other five VY8 variants up to a 100-μM concentration (Fig. 4*A*). In TCR-231, RY11-8A showed the most profound response, whereas RY11-3A and RY11-4A had reactivity comparable to that of RY11 (Fig. 4*B*). However, RY11-9A showed weak reactivity; and the other seven RY11 variants had no reactivity (Fig. 4*B*). We also tested various amino acid variations (57 variant peptides in total) for their reactivity toward TCR-139 and TCR-231 (data not shown), but VY8-5A and RY11-8A showed the most pronounced effects on IL-2 production by TCR-transduced T cells.

Next, we examined the decay of a series of alanine variant peptides from HLA-B35. The pMHC decay of VY8-5A and VY8-3A was substantially delayed with a half-life of $>4 \times 10^3$ min, whereas the half-life of VY8-1A was slightly more rapid with one of $2.0 \pm 0.80 \times 10^2$ min (Fig. 4*C*). None of the other VY8 variants showed any reactivity (Fig. 4*C*), consistent with the data obtained under the no-wash condition (Fig. 4*A*). Among the RY11 variants, the decay of RY11-8A was substantially delayed with a half-life of $2.7 \pm 0.44 \times 10^3$ min, whereas that of RY11-3A, RY11-4A, and RY11-9A was slightly delayed with half lives of $2.5 \pm 0.44 \times 10^2$, $2.0 \pm 0.40 \times 10^2$, and $2.2 \pm 0.40 \times 10^2$ min, respectively (Fig. 4*D*). None of the other RY11 variants showed any reactivity (Fig. 4*D*), consistent with the data from the no-wash condition (Fig. 4*B*). Taken together, VY8-5A and RY11-8A provided the most profound effects on pMHC decay and T cell stimulation among the wild-type and variant peptides examined.

Enhancement of susceptibility of Nef variant-expressing cells to CTL killing

To ask whether the variant Ags can improve the susceptibility to killing by CTLs, we took advantage of the fact that the alanine substitution at Pro^{82} of Nef_{SF2} resulted in the generation of both

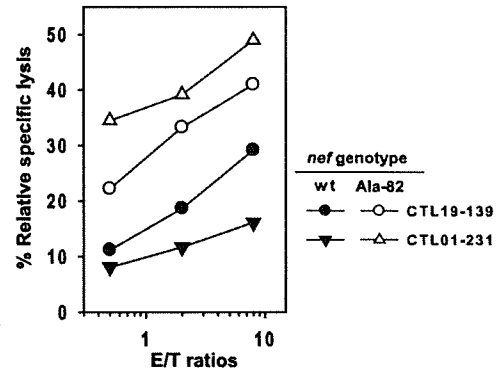

FIGURE 5. Effect of an amino acid substitution on CTL killing of Nef-expressing cells. Primary $CD4^+$ cells isolated from an HIV-negative donor (*HLA-B*3501*$^+$) were transfected with a gene encoding GFP alone, wild-type, or the Ala^{82} mutant of Nef_{SF2}-GFP fusion protein, and then mixed with CTL 19-139 or CTL 01-231 at the indicated E:T ratios. The transfection efficiency was 60 ± 5% as determined by GFP expression. Cytotoxic activity toward cells expressing GFP alone was always <10%. Data are the means of duplicate assays, An independent experiment using another PBMC donor and another set of CTL clones gave similar results.

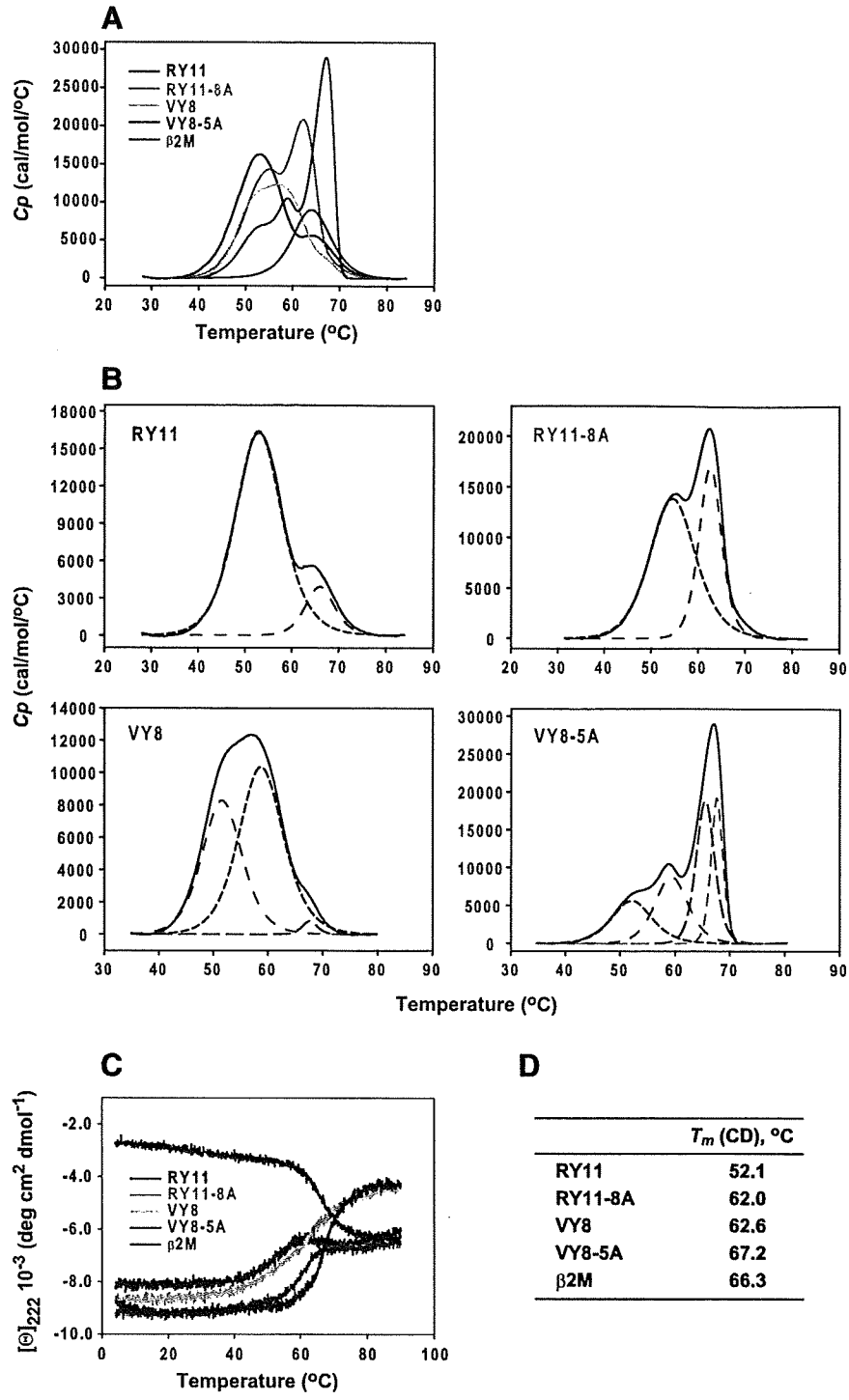

FIGURE 6. Thermostability analysis of peptide-HLA-B35 complexes. *A* and *B*, DSC analysis of pMHC complexes. *A*, The excessive heat capacity of β_2m alone and that of HLA-B35 in complex with indicated peptides was measured by DSC analysis. *B*, Deconvolution of the experimental curves (solid line histogram) of HLA-B35 in complex with the indicated peptides. Deconvolution results in two-state transitions (broken line histogram). T_m and ΔH_m values obtained are given in Table I. *C* and *D*, CD analysis of pMHC complexes. The ellipticity (as θ) at 222 nm of β_2m alone and that of HLA-B35 in complex with the indicated peptides was measured by CD analysis (*C*). The CD melting temperatures, T_m (CD), are also shown (*D*).

VY8-5A and RY11-8A variant Ags. Primary $CD4^+$ cells were transfected with the wild-type or the Ala^{82} variant *nef* genes. The cells with the Ala^{82} variant showed substantially increased susceptibility to killing by both CTL 19-139 and CTL 01-231 (Fig. 5), suggesting that the variant antigenic peptides with slower pMHC decay rendered HIV-infected cells more susceptible to CTL-mediated viral containment.

Thermostability analysis of pMHC

To characterize the biochemical differences between VY8/HLA-B35 and RY11/HLA-B35 complexes, we analyzed the thermostability of free β_2m and that of these heterotrimers (composed of β_2m, H chain, and peptide) by DSC. The heat capacity curve of β_2m, a protein composed of a stable domain containing exclusively β strands, showed a single two-state transition at T_m of 64.18°C (Fig. 6*A* and Table I), in good agreement with a previous report (36). In contrast, the heat capacity curve of RY11/HLA-B35 was characterized by two partly overlapping peaks with the melting temperature of the first peak (T_m^1) substantially below that of β_2m (Fig. 6, *A* and *B* and Table I). The other single transition at the high temperature peak appeared to result from the melting of β_2m, as the T_m^2 value of RY11/HLA-B35 was comparable to that of free β_2m (Table I). These results suggest that the melting of RY11/HLA-B35 started with unfolding of the H chain and concomitant

Table I. *DSC measurements of pMHC complexes*

Sample	Transition Temperature, T_m (°C)				Calorimetric Enthalpy, ΔH_m (kcal/mol)				
	T_m^1	T_m^2	T_m^3	T_m^4	ΔH_m^1	ΔH_m^2	ΔH_m^3	ΔH_m^4	ΔH_{tot}
VY8/HLA35	51.66 ± 0.06	58.83 ± 0.055	67.72 ± 0.087	N/A	80.72	112.7	2.9	N/A	196.32
VY8-5A/HLA35	52.22 ± 0.36	59.42 ± 0.13	65.57 ± 0.3	67.71 ± 0.10	55.44	70.52	84.63	55.6	266.19
RY11/HLA35	52.07 ± 0.019	66.10 ± 0.068	N/A	N/A	215.1	32.16	N/A	N/A	247.26
RY11-8A/HLA35	54.68 ± 0.065	62.56 ± 0.013	N/A	N/A	178.8	108.6	N/A	N/A	287.40
β_2m	64.18 ± 0.0031	N/A	N/A	N/A	96.9	N/A	N/A	N/A	96.9

N/A, Not applicable.

release of folded β_2m, which subsequently melted at the higher temperature.

In contrast, the heat capacity curve of VY8/HLA-B35 appeared to be quite different from that of the RY11 counterpart, as the deconvolution of the VY8/HLA-B35 experimental heat capacity profile showed three peaks, which heavily overlapped each other and were less well separated (Fig. 6, *A* and *C* and Table I). The transition of the third peak, which was separated by a shoulder at the high temperature side of the second peak (Fig. 6*C*), could be correlated with the melting of β_2m, as both melting temperatures were comparable, although interestingly, the ΔH_m^3 value of VY8/HLA-B35 was much lower than that of free β_2m (Table I). The melting of the H chain of VY8/HLA-B35 could not be annotated on a single transition, either T_m^1 or T_m^2. Rather, the results suggested that the melting of the entire VY8/HLA-B35 complex occurred simultaneously and cooperatively with the H chain and β_2m.

To examine the contribution of peptides on the thermostability profile of pMHC, we also analyzed RY11-8A and VY8-5A in complex with HLA-B35 by DSC. Both single mutations showed substantial effects on the heat capacity profiles of overall pMHC complexes and increased total enthalpy values compared with those of their respective wild-type counterparts (Fig. 6, *A*, *D*, and *E* and Table I). Notably, transitions at high temperature peaks in the variant peptide complexes, corresponding to T_m^2 for RY11-8A/HLA-B35 and T_m^3 or T_m^4 for VY8-5A/HLA-B35, appeared to rely on a contribution from β_2m, although these enthalpy costs were considerably larger than the enthalpy change of free β_2m (Table I), suggesting a substantial contribution from the H chain to these transitions.

To further examine the contribution of peptides on the thermostability profile of pMHC, we obtained CD profiles of these pMHC heterotrimers to see the thermally induced changes in their secondary structures. We observed substantial differences in CD profiles between β_2m alone and all pMHC heterotrimers examined (Fig. 6*C*). β_2m alone melted with T_m in the CD analysis of 66.3°C (Fig. 6*D*), in good agreement with the T_m^1 value in the DSC analysis (Table I) as well as with a previous report (36). In contrast, all pMHC heterotrimers had much larger negative molar ellipticity at 222 nm at a low temperature range than β_2m alone (Fig. 6*C*), most likely reflecting the presence of α helices in their H chain subunits. In addition, each pMHC complex showed a different reduction in their negative molar ellipticity with increasing temperatures (Fig. 6*C*), highlighting the contribution of peptides on the thermostability of the secondary structure in their H chain subunits. Specifically, RY11/HLA-B35 melted with a T_m (CD) of 52.1°C (Fig. 6*D*), a value consistent with the T_m^1 in the DSC analysis, confirming the observation made by DSC that melting of RY11/HLA-B35 started with unfolding of the H chain subunit. In addition, VY8/HLA-B35 melted at a much higher temperature (Fig. 6*D*) than RY11/HLA-B35, confirming the potent thermostability of the VY8/HLA-B35 complex as observed in the DSC analysis. Finally, the HLA-B35 complexes with the variant peptides melted at higher temperatures than their wild-type counterparts (Fig. 6, *C* and *D*), confirming again the contribution of variant peptides on the profound thermostability in these pMHC complexes as observed in DSC analysis.

Discussion

In the present study, using TCR-reconstructed cells we clearly showed that the difference in antiviral cytotoxic activity between mature CTLs specific for two different but closely related antigenic Nef peptides (VY8 and RY11) was not caused by the difference in functional avidity of TCR-pMHC interactions. Rather, our data demonstrated that the antiviral activity of these effector CTLs was much influenced by peptide intrinsic factors including peptide-off rate and cooperative thermodynamics of the cognate pMHC. The data obtained by introduction of a mutation in the Nef protein that resulted in the alteration of both epitopes to VY8-5A and RY11-8A further confirmed the association between these peptide intrinsic factors and the susceptibility of Nef-expressing cells to killing by the cognate CTLs. Our results are partly in line with those of previous studies demonstrating that the peptide-off rate of pMHC is an important factor for generating immunodominance hierarchy in class I (34, 37–39) and class II (40, 41) MHC-restricted T cell responses, i.e., the slower the peptide-off rate, the greater the abundance of a given pMHC on the surface of APCs, which leads to the generation of immunodominant T cell responses (26). However, immunodominant peptides are not always those with the highest density presented at the target cell surface (23, 24), and immunodominant CTLs do not always play a dominant role in containment of HIV replication (25). The results shown here extend these previous findings that interdependent and cooperative thermostability profiles of pMHC induced by antigenic peptides can be associated with efficient recognition by CTLs for killing virus-infected target cells.

The DSC and CD measurements showed significantly different thermostability profiles among HLA-B35 in complex with VY8, RY11, and their variant peptides. In comparison of the thermostability of HLA-B35 complexes between wild-type peptides and their variants, we found significant effects of the mutations on thermal stabilization of the entire pMHC, as the total enthalpy values required for unfolding of HLA-B35 in complex with the variant peptides were substantially increased compared with those for their respective wild-type counterpart. This thermal stabilization by the variant peptide was corroborated by the DSC and CD analyses and is most likely associated with slow dissociation of these peptides from pMHC, as observed in the cell-based assays. In contrast, the calorimetric unfolding enthalpy of RY11/HLA-B35 obtained by deconvolution of the experimental heat capacity curve was higher than that of its VY8 counterpart, although the cell-based assays showed rapid dissociation of RY11 from pMHC. In this regard, it is possible that RY11 and HLA-B35 may bind with multiple different conformations; because relatively long

peptides can be accommodated on the peptide binding groove of HLA class I molecules with their central region bulged (42–45) or either end extended away (46). This result is less likely in this study, however, because TCR-231-transduced cells responded to target cells pulsed with RY11 but not to those with truncated peptides such as VY8 and RM9 (RPQVPLRPM, data not shown). Also, the HLA-B35 tetramers prepared with RY11 showed binding exclusively with TCR-231 but not with other TCRs including VY8-specific TCR-139. It is also conceivable that the peptide-off rate from the membrane-bound and glycosylated form of pMHC (i.e., present on the cell surface) is not correlated with the thermostability of the soluble form of pMHC (i.e., using bacterially produced extracellular domain). Alternatively, peptides that are endogenously loaded onto the empty MHC class I with the assistance of a specialized multimeric unit called the peptide-loading complex (47, 48) in the endoplasmic reticulum could have conformational characteristics different from those of molecules refolded in vitro. More importantly, the RY11/HLA-B35 complex showed two relatively simple two-state transitions in thermal unfolding, in which a high-temperature transition corresponds to free β_2m. Such an unfolding pattern has been reported for various self-peptides in association with HLA-B27 (36, 49). In contrast, the VY8/HLA-B35 complex and two other variant complexes showed significantly interdependent and cooperative unfolding processes among heterotrimer subunits and structural domains, suggesting the critical contribution of β_2m in maintaining antigenicity of the peptide in association with the H chain. However, whether such a conformational characteristic in a given pMHC can be directly attributable to efficient docking by cognate TCRs, to preferential loading of peptides in an intracellular peptide selection process, or to both events needs to be examined by further intense experiments.

In HIV-infected cells, antigenic peptides are generated through the endogenous MHC class I Ag processing and presentation pathway for CTL recognition. Peptides generated in the cytosol mainly by the proteasome are translocated into the endoplasmic reticulum by mediation of the TAP, and then loaded onto the empty MHC class I (47, 50). It has been reported that sequence specificities by TAP can influence the efficiency of epitope presentation by cell surface MHC class I molecules (47, 50, 51). It is therefore conceivable that the increased susceptibility of Nef-expressing cells to CTL recognition by the Ala^{82} mutation observed in our study might be attributable to the enhancement of the TAP efficiency, in addition to peptide intrinsic factors including peptide-off rate and thermodynamics of the cognate pMHC. However, this scenario is less likely because it is well known that the amino acid substitutions in the middle of epitopes, such as VY8-5A and RY11-8A in our study, have only a limited effect on TAP efficiency (52–54). Considering that a number of human viruses including HIV-1 can somehow abrogate the TAP function (50, 55), how the TAP efficiency influences the susceptibility of cells infected with various variant viruses to CTL killing is an important question to be addressed in future studies.

Both VY8 and RY11 share anchor residues, proline at position 2 and tyrosine at the C terminus, which are optimal for binding with HLA-B*3501 (56, 57); and both Ags are dominantly recognized in *HLA-B*3501*$^+$ individuals with an HIV-1 infection (6, 10, 58). Even in such a case, the improved thermostability of pMHC by an amino acid substitution within the epitopes, even other than a primary anchor residue, can substantially enhance the susceptibility to recognition by CTLs for killing target cells, suggesting that the altered peptide ligand strategy is capable of enhancing CTL-mediated immune responses against HIV-1 infection similar to that used for anti-cancer vaccines targeting self-Ags (34, 39). Our data thus highlight the importance of incorporating thermostability data in the process of rational optimization of Ags that support profound antiviral activity by HIV-specific CTLs.

Acknowledgments

We thank S. Dohki, Y. Idegami, and T. Akahoshi for excellent technical help.

Disclosures

The authors have no financial conflict of interest.

References

1. Migueles, S. A., A. C. Laborico, W. L. Shupert, M. S. Sabbaghian, R. Rabin, C. W. Hallahan, D. Van Baarle, S. Kostense, F. Miedema, M. McLaughlin, et al. 2002. HIV-specific CD8$^+$ T cell proliferation is coupled to perforin expression and is maintained in nonprogressors. *Nat. Immunol.* 3: 1061–1068.
2. Saez-Cirion, A., C. Lacabaratz, O. Lambotte, P. Versmisse, A. Urrutia, F. Boufassa, F. Barre-Sinoussi, J.-F. Delfraissy, M. Sinet, G. Pancino, et al. 2007. HIV controllers exhibit potent CD8 T cell capacity to suppress HIV infection ex vivo and peculiar cytotoxic T lymphocyte activation phenotype. *Proc. Natl. Acad. Sci. USA* 104: 6776–6781.
3. Yang, O. O., S. A. Kalams, A. Trocha, H. Cao, A. Luster, R. P. Johnson, and B. D. Walker. 1997. Suppression of human immunodeficiency virus type 1 replication by CD8$^+$ cells: evidence for HLA class I-restricted triggering of cytolytic and noncytolytic mechanisms. *J. Virol.* 71: 3120–3128.
4. Kiepiela, P., K. Ngumbela, C. Thobakgale, D. Ramduth, I. Honeyborne, E. Moodley, S. Reddy, C. de Pierres, Z. Mncube, N. Mkhwanazi, et al. 2007. CD8$^+$ T-cell responses to different HIV proteins have discordant associations with viral load. *Nat. Med.* 13: 46–53.
5. Tomiyama, H., M. Fujiwara, S. Oka, and M. Takiguchi. 2005. Epitope-dependent effect of Nef-mediated HLA class I down-regulation on ability of HIV-1-specific CTLs to suppress HIV-1 replication. *J. Immunol.* 174: 36–40.
6. Ueno, T., Y. Idegami, C. Motozono, S. Oka, and M. Takiguchi. 2007. Altering effects of antigenic variations in HIV-1 on antiviral effectiveness of HIV-specific CTLs. *J. Immunol.* 178: 5513–5523.
7. Yang, O. O., P. T. N. Sarkis, A. Trocha, S. A. Kalams, R. P. Johnson, and B. D. Walker. 2003. Impacts of avidity and specificity on the antiviral efficiency of HIV-1-specific CTL. *J. Immunol.* 171: 3718–3724.
8. Goulder, P. J. R., M. A. Altfeld, E. S. Rosenberg, T. Nguyen, Y. Tang, R. L. Eldridge, M. M. Addo, S. He, J. S. Mukherjee, M. N. Phillips, et al. 2001. Substantial differences in specificity of HIV-specific cytotoxic T cells in acute and chronic HIV infection. *J. Exp. Med.* 193: 181–194.
9. Lichterfeld, M., X. G. Yu, D. Cohen, M. M. Addo, J. Malenfant, B. Perkins, E. Pae, M. N. Johnston, D. Strick, T. M. Allen, et al. 2004. HIV-1 Nef is preferentially recognized by CD8 T cells in primary HIV-1 infection despite a relatively high degree of genetic diversity. *AIDS* 18: 1383–1392.
10. Ueno, T., C. Motozono, S. Douki, P. Mwimanzi, S. Rauch, O. T. Fackler, S. Oka, and M. Takiguchi. 2008. CTL-mediated selective pressure influences dynamic evolution and pathogenic functions of HIV-1 Nef. *J. Immunol.* 180: 1107–1116.
11. Goulder, P. J. R., and D. I. Watkins. 2004. HIV and SIV CTL escape: implications for vaccine design. *Nat. Rev. Immunol.* 4: 630–640.
12. Nowak, M. A., R. M. May, R. E. Phillips, S. Rowland-Jones, D. G. Lalloo, S. McAdam, P. Klenerman, B. Koppe, K. Sigmund, C. R. M. Bangham, and A. J. McMichael. 1995. Antigenic oscillations and shifting immunodominance in HIV-1 infections. *Nature* 375: 606–611.
13. Almeida, J. R., D. A. Price, L. Papagno, Z. A. Arkoub, D. Sauce, E. Bornstein, T. E. Asher, A. Samri, A. Schnuriger, I. Theodorou, et al. 2007. Superior control of HIV-1 replication by CD8$^+$ T cells is reflected by their avidity, polyfunctionality, and clonal turnover. *J. Exp. Med.* 204: 2473–2485.
14. Dong, T., G. Stewart-Jones, N. Chen, P. Easterbrook, X. Xu, L. Papagno, V. Appay, M. Weekes, C. Conlon, C. Spina, et al. 2004. HIV-specific cytotoxic T cells from long-term survivors select a unique T cell receptor. *J. Exp. Med.* 200: 1547–1557.
15. Ueno, T., H. Tomiyama, M. Fujiwara, S. Oka, and M. Takiguchi. 2004. Functionally impaired HIV-specific CD8 T cells show high affinity TCR-ligand interactions. *J. Immunol.* 173: 5451–5457.
16. Turnbull, E. L., A. R. Lopes, N. A. Jones, D. Cornforth, P. Newton, D. Aldam, P. Pellegrino, J. Turner, I. Williams, C. M. Wilson, et al. 2006. HIV-1 epitope-specific CD8$^+$ T cell responses strongly associated with delayed disease progression cross-recognize epitope variants efficiently. *J. Immunol.* 176: 6130–6146.
17. Ali, A., R. Lubong, H. Ng, D. G. Brooks, J. A. Zack, and O. O. Yang. 2004. Impacts of epitope expression kinetics and class I downregulation on the antiviral activity of human immunodeficiency virus type 1-specific cytotoxic T lymphocytes. *J. Virol.* 78: 561–567.
18. Sacha, J. B., C. Chung, E. G. Rakasz, S. P. Spencer, A. K. Jonas, A. T. Bean, W. Lee, B. J. Burwitz, J. J. Stephany, J. T. Loffredo, et al. 2007. Gag-specific CD8$^+$ T lymphocytes recognize infected cells before AIDS-virus integration and viral protein expression. *J. Immunol.* 178: 2746–2754.
19. van Baalen, C. A., C. Guillon, M. van Baalen, E. J. Verschuren, P. H. Boers, A. D. Osterhaus, and R. A. Gruters. 2002. Impact of antigen expression kinetics on the effectiveness of HIV-specific cytotoxic T lymphocytes. *Eur. J. Immunol.* 32: 2644–2652.
20. Le Gall, S., P. Stamegna, and B. D. Walker. 2007. Portable flanking sequences modulate CTL epitope processing. *J. Clin. Invest.* 117: 3563–3575.

21. Lichterfeld, M., X. G. Yu, S. Le Gall, and M. Altfeld. 2005. Immunodominance of HIV-1-specific CD8$^+$ T-cell responses in acute HIV-1 infection: at the crossroads of viral and host genetics. *Trends Immunol.* 26: 166–171.
22. Sette, A., A. Vitiello, B. Reherman, P. Fowler, R. Nayersina, W. M. Kast, C. J. Melief, C. Oseroff, L. Yuan, and J. Ruppert. 1994. The relationship between class I binding affinity and immunogenicity of potential cytotoxic T cell epitopes. *J. Immunol.* 153: 5586–5592.
23. Bihl, F., N. Frahm, L. Di Giammarino, J. Sidney, M. John, K. Yusim, T. Woodberry, K. Sango, H. S. Hewitt, L. Henry, et al. 2006. Impact of HLA-B alleles, epitope binding affinity, functional avidity, and viral coinfection on the immunodominance of virus-specific CTL responses. *J. Immunol.* 176: 4094–4101.
24. Crotzer, V. L., R. E. Christian, J. M. Brooks, J. Shabanowitz, R. E. Settlage, J. A. Marto, F. M. White, A. B. Rickinson, D. F. Hunt, and V. H. Engelhard. 2000. Immunodominance among EBV-derived epitopes restricted by HLA-B27 does not correlate with epitope abundance in EBV-transformed B-lymphoblastoid cell lines. *J. Immunol.* 164: 6120–6129.
25. Frahm, N., P. Kiepiela, S. Adams, C. H. Linde, H. S. Hewitt, K. Sango, M. E. Feeney, M. M. Addo, M. Lichterfeld, M. P. Lahaie, et al. 2006. Control of human immunodeficiency virus replication by cytotoxic T lymphocytes targeting subdominant epitopes. *Nat. Immunol.* 7: 173–178.
26. Yewdell, J. W. 2006. Confronting complexity: real-world immunodominance in antiviral CD8$^+$ T cell responses. *Immunity* 25: 533–543.
27. Ueno, T., H. Tomiyama, M. Fujiwara, S. Oka, and M. Takiguchi. 2003. HLA class I-restricted recognition of an HIV-derived epitope peptide by a human T cell receptor α chain having a Vδ1 variable segment. *Eur. J. Immunol.* 33: 2910–2916.
28. Ueno, T., H. Tomiyama, and M. Takiguchi. 2002. Single T cell receptor-mediated recognition of an identical HIV-derived peptide presented by multiple HLA class I molecules. *J. Immunol.* 169: 4961–4969.
29. Kessels, H. W., M. D. van den Boom, H. Spits, E. Hooijberg, and T. N. M. Schumacher. 2000. Changing T cell specificity by retroviral T cell receptor display. *Proc. Natl. Acad. Sci. USA* 97: 14578–14583.
30. Yokosuka, T., K. Takase, M. Suzuki, Y. Nakagawa, S. Taki, H. Takahashi, T. Fujisawa, H. Arase, and T. Saito. 2002. Predominant role of T cell receptor (TCR)-α chain in forming preimmune TCR repertoire revealed by clonal TCR reconstitution system. *J. Exp. Med.* 195: 991–1001.
31. Day, C. L., D. E. Kaufmann, P. Kiepiela, J. A. Brown, E. S. Moodley, S. Reddy, E. W. Mackey, J. D. Miller, A. J. Leslie, C. DePierres, et al. 2006. PD-1 expression on HIV-specific T cells is associated with T-cell exhaustion and disease progression. *Nature* 443: 350–354.
32. Jones, R. B., L. C. Ndhlovu, J. D. Barbour, P. M. Sheth, A. R. Jha, B. R. Long, J. C. Wong, M. Satkunarajah, M. Schweneker, J. M. Chapman, et al. 2008. Tim-3 expression defines a novel population of dysfunctional T cells with highly elevated frequencies in progressive HIV-1 infection. *J. Exp. Med.* 205: 2763–2779.
33. Trautmann, L., L. Janbazian, N. Chomont, E. A. Said, S. Gimmig, B. Bessette, M.-R. Boulassel, E. Delwart, H. Sepulveda, R. S. Balderas, et al. 2006. Upregulation of PD-1 expression on HIV-specific CD8$^+$ T cells leads to reversible immune dysfunction. *Nat. Med.* 12: 1198–1202.
34. Borbulevych, O. Y., T. K. Baxter, Z. Yu, N. P. Restifo, and B. M. Baker. 2005. Increased immunogenicity of an anchor-modified tumor-associated antigen is due to the enhanced stability of the peptide/MHC complex: implications for vaccine design. *J. Immunol.* 174: 4812–4820.
35. Fischer, A., S. Latour, and G. de Saint Basile. 2007. Genetic defects affecting lymphocyte cytotoxicity. *Curr. Opin. Immunol.* 19: 348–353.
36. Hillig, R. C., M. Hulsmeyer, W. Saenger, K. Welfle, R. Misselwitz, H. Welfle, C. Kozerski, A. Volz, B. Uchanska-Ziegler, and A. Ziegler. 2004. Thermodynamic and structural analysis of peptide- and allele-dependent properties of two HLA-B27 subtypes exhibiting differential disease association. *J. Biol. Chem.* 279: 652–663.
37. Elliott, T., and A. Williams. 2005. The optimization of peptide cargo bound to MHC class I molecules by the peptide-loading complex. *Immunol. Rev.* 207: 89–99.
38. van der Burg, S. H., M. J. Visseren, R. M. Brandt, W. M. Kast, and C. J. Melief. 1996. Immunogenicity of peptides bound to MHC class I molecules depends on the MHC-peptide complex stability. *J. Immunol.* 156: 3308–3314.
39. Yu, Z., M. R. Theoret, C. E. Touloukian, D. R. Surman, S. C. Garman, L. Feigenbaum, T. K. Baxter, B. M. Baker, and N. P. Restifo. 2004. Poor immunogenicity of a self/tumor antigen derives from peptide-MHC-I instability and is independent of tolerance. *J. Clin. Invest.* 114: 551–559.
40. Lazarski, C. A., F. A. Chaves, S. A. Jenks, S. Wu, K. A. Richards, J. M. Weaver, and A. J. Sant. 2005. The kinetic stability of MHC class II:peptide complexes is a key parameter that dictates immunodominance. *Immunity* 23: 29–40.
41. Sant, A. J., F. A. Chaves, S. A. Jenks, K. A. Richards, P. Menges, J. M. Weaver, and C. A. Lazarski. 2005. The relationship between immunodominance, DM editing, and the kinetic stability of MHC class II:peptide complexes. *Immunol. Rev.* 207: 261–278.
42. Burrows, J. M., M. J. Bell, R. Brennan, J. J. Miles, R. Khanna, and S. R. Burrows. 2008. Preferential binding of unusually long peptides to MHC class I and its influence on the selection of target peptides for T cell recognition. *Mol. Immunol.* 45: 1818–1824.
43. Green, K. J., J. J. Miles, J. Tellam, W. J. van Zuylen, G. Connolly, and S. R. Burrows. 2004. Potent T cell response to a class I-binding 13-mer viral epitope and the influence of HLA micropolymorphism in controlling epitope length. *Eur. J. Immunol.* 34: 2510–2519.
44. Probst-Kepper, M., H. J. Hecht, H. Herrmann, V. Janke, F. Ocklenburg, J. Klempnauer, B. J. van den Eynde, and S. Weiss. 2004. Conformational restraints and flexibility of 14-meric peptides in complex with HLA-B*3501. *J. Immunol.* 173: 5610–5616.
45. Probst-Kepper, M., V. Stroobant, R. Kridel, B. Gaugler, C. Landry, F. Brasseur, J. P. Cosyns, B. Weynand, T. Boon, and B. J. Van Den Eynde. 2001. An alternative open reading frame of the human macrophage colony-stimulating factor gene is independently translated and codes for an antigenic peptide of 14 amino acids recognized by tumor-infiltrating CD8 T lymphocytes. *J. Exp. Med.* 193: 1189–1198.
46. Collins, E. J., D. N. Garboczi, and D. C. Wiley. 1994. Three-dimensional structure of a peptide extending from one end of a class I MHC binding site. *Nature* 371: 626–629.
47. Raghavan, M., N. Del Cid, S. M. Rizvi, and L. R. Peters. 2008. MHC class I assembly: out and about. *Trends Immunol.* 29: 436–443.
48. Wearsch, P. A., and P. Cresswell. 2008. The quality control of MHC class I peptide loading. *Curr. Opin. Cell Biol.* 20: 624–631.
49. Hulsmeyer, M., K. Welfle, T. Pohlmann, R. Misselwitz, U. Alexiev, H. Welfle, W. Saenger, B. Uchanska-Ziegler, and A. Ziegler. 2005. Thermodynamic and structural equivalence of two HLA-B27 subtypes complexed with a self-peptide. *J. Mol. Biol.* 346: 1367–1379.
50. Abele, R., and R. Tamp. 2006. Modulation of the antigen transport machinery TAP by friends and enemies. *FEBS Letters* 580: 1156–1163.
51. Garbi, N., S. Tanaka, M. van den Broek, F. Momburg, and G. J. Hammerling. 2005. Accessory molecules in the assembly of major histocompatibility complex class I/peptide complexes: how essential are they for CD8$^+$ T-cell immune responses? *Immunol. Rev.* 207: 77–88.
52. Daniel, S., V. Brusic, S. Caillat-Zucman, N. Petrovsky, L. Harrison, D. Riganelli, F. Sinigaglia, F. Gallazzi, J. Hammer, and P. M. van Endert. 1998. Relationship between peptide selectivities of human transporters associated with antigen processing and HLA class I molecules. *J. Immunol.* 161: 617–624.
53. Peters, B., S. Bulik, R. Tampe, P. M. van Endert, and H.-G. Holzhutter. 2003. Identifying MHC class I epitopes by predicting the TAP transport efficiency of epitope precursors. *J. Immunol.* 171: 1741–1749.
54. Schatz, M. M., B. Peters, N. Akkad, N. Ullrich, A. N. Martinez, O. Carroll, S. Bulik, H.-G. Rammensee, P. van Endert, H.-G. Holzhutter, et al. 2008. Characterizing the N-terminal processing motif of MHC class I ligands. *J. Immunol.* 180: 3210–3217.
55. Kutsch, O., T. Vey, T. Kerkau, T. Hunig, and A. Schimpl. 2002. HIV type 1 abrogates TAP-mediated transport of antigenic peptides presented by MHC class I. *AIDS Res. Hum. Retroviruses* 18: 1319–1325.
56. Rammensse, H.-G., T. Friede, and S. Stevanovic. 1995. MHC ligands and peptide motifs: first listing. *Immunogenetics* 41: 178–228.
57. Smith, K. J., S. W. Reid, D. I. Stuart, A. J. McMichael, E. Y. Jones, and J. I. Bell. 1996. An altered position of the α2 helix of MHC class I is revealed by the crystal structure of HLA-B*3501. *Immunity* 4: 203–213.
58. Rowland-Jones, S., J. Sutton, K. Ariyoshi, T. Dong, F. Gotch, S. McAdam, D. Whitby, S. Sabally, A. Gallimore, T. Corrah, et al. 1995. HIV-specific cytotoxic T-cells in HIV-exposed but uninfected Gambian women. *Nat. Med.* 1: 59–64.